

# DESIGN OF A NOVEL EBG SURFACE FOR THE PERFORMANCE ENHANCEMENT OF PRINTED ANTENNAS

## A DISSERTATION

*Submitted in partial fulfillment of the  
requirements for the award of the degree*

*of*

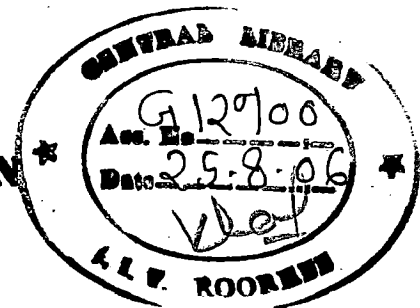
**MASTER OF TECHNOLOGY**

*in*

**ELECTRONICS AND COMMUNICATION ENGINEERING  
(With Specialization in RF and Microwave Engineering)**

By

**MANISH JAIN** \*



**DEPARTMENT OF ELECTRONICS AND COMPUTER ENGINEERING  
INDIAN INSTITUTE OF TECHNOLOGY ROORKEE  
ROORKEE-247 667 (INDIA)**

**JUNE, 2006**

*LP*

## CANDIDATE'S DECLARATION

I hereby declare that the work, which is being presented in the dissertation entitled “**Design of a Novel EBG Surface for the Performance Enhancement of Printed Antennas**”, which is submitted in the partial fulfillment of the requirements for the award of degree of **Master of Technology in RF & Microwave Engineering**, submitted in the Department of Electronics and Computer Engineering, **Indian Institute of Technology – Roorkee**, Roorkee (INDIA), is an authentic record of my own work carried out under the guidance of **Dr. S. N. Sinha**, Professor and **Dr. S. Pal**, Assistant Professor, Department of Electronics and Computer Engineering, Indian Institute of Technology, Roorkee.


I have not submitted the matter embodied in this dissertation for the award of any other degree or diploma.

Dated : 29/06/2006  
Place: Roorkee


  
(Manish Jain)

## CERTIFICATE

This is to certify that the above statements made by the student are correct to the best of our knowledge.



(Dr. S. N. Sinha )  
Professor  
Dept. of E & C Engg.  
IIT-R, Roorkee – 247667,  
INDIA.



(Dr. S. Pal)  
Assistant Professor  
Dept. of E & C Engg.  
IIT-R, Roorkee – 247667,  
INDIA.

## ACKNOWLEDGEMENT

---

---

It gives me great pleasure to take this opportunity to thank and express my deep sense of gratitude to my guides Dr. S. N. Sinha, Professor and Dr. S. Pal, Assistant Professor, Department of Electronics and Computer Engineering, Indian Institute of Technology – Roorkee for their invaluable guidance through out the period of this dissertation work. Further I am thankful to them for all the inspiration and motivation they inculcated in me.

I express my sincere thanks to Dr. B. Sinha, Emeritus Fellow, Dr. N. K. Agrawal, Emeritus Fellow, Dr. M. V. Kartikeyan, Associate Professor and Dr. D. Singh, Assistant Professor, Department of Electronics and Computer Engineering, Indian Institute of Technology - Roorkee for their kind help, moral support and for all I have learned from them directly or indirectly in class room contact hours or at other times.

I am obliged to the H.O.D. of Department of Electronics & Computer Engineering for creating the right infrastructure and facilities conducive to this work in the department.

I would like to thank the staff of Advance Microwave Laboratory Mr. Raja Ram, Mr. Lakhan Giri and Mr. Veer Singh for their help to carry out this dissertation work in the Laboratory.

My special sincere heartfelt gratitude to my family, whose sincere prayer, best wishes, support and unflinching encouragement has been a constant source of strength to me during the entire work.

Finally I would thank all my friends and classmates for their support and valuable suggestions.



( **Manish Jain** )

## ABSTRACT

---

---

A novel cross shaped electromagnetic structure is developed that is characterized by high surface impedance and which behaves as an Electromagnetic Band Gap structure. Parametric studies have been performed to obtain design guidelines for the EBG structure and it is then optimized for operation at C band. Three techniques, including analytical and simulation techniques, have been employed to find and confirm the band gap of the structure. The designed EBG has been employed for performance enhancement in various applications. It has been employed for reducing the mutual coupling between the elements of a 2x1 microstrip patch antenna array. The designed EBG is also employed as reflector for dipole and slot antennas to reduce the profile and increase in the gain of these antennas. All this work has been done using simulations on Zeland's IE3D simulation software.

## TABLE OF CONTENTS

|  |            |
|--|------------|
| <b>CANDIDATE'S DECLARATION</b>                                       | <b>i</b>   |
| <b>CERTIFICATE</b>   | <b>i</b>   |
| <b>ACKNOWLEDGEMENT</b>   | <b>ii</b>  |
| <b>ABSTRACT</b>  | <b>iii</b> |
| <b>1. INTRODUCTION</b>   | <b>1</b>   |
| 1.1. Electromagnetic Band Gap Structures                             | 1          |
| 1.2. Need for Electromagnetic Band Gap Structures                    | 2          |
| 1.3. Literature survey   | 4          |
| 1.4. Motivation and Scope  | 9          |
| 1.5. Problem Statement   | 10         |
| 1.6. Organization of the Dissertation                                | 10         |
| <b>2. DESIGN AND PARAMETRIC STUDY OF THE PROPOSED EBG STRUCTURE</b>  | <b>12</b>  |
| 2.1. Working Principle of EBG structure                              | 12         |
| 2.2. A Corrugated Surface approach to EBG                            | 14         |
| 2.3. Proposed EBG structure  | 15         |
| 2.4. Parametric study of the EBG surface                             | 17         |
| 2.5. Optimized Parameters of the proposed EBG structure              | 23         |
| 2.6. Band Gap determination method of the EBG structure              | 24         |
| <b>3. MUTUAL COUPLING REDUCTION BETWEEN ARRAY ELEMENTS USING EBG</b> | <b>29</b>  |
| 3.1. Mutual Coupling Comparison Of Various Microstrip Antenna Arrays | 30         |
| 3.2. Mutual Coupling Reduction Using The EBG Structure               | 35         |
| 3.3. Effect of EBG cell matrix variation on mutual coupling          | 37         |

|   |           |
|---|-----------|
| <b>4. EFFECT OF THE PROPOSED EBG SURFACE ON THE RADIATION CHARACTERISTICS OF A DIPOLE ANTENNA</b> | <b>42</b> |
| <b>4.1. Comparison of the PEC, Free Space and EBG Ground Planes</b>                               | <b>42</b> |
| <b>5. EFFECT OF EBG SURFACE ON THE RADIATION CHARACTERISTICS OF A MICROSTRIP SLOT ANTENNA</b>     | <b>49</b> |
| <b>5.1. Rectangular-slot antenna</b>  | <b>50</b> |
| <b>5.2. EBG backed Rectangular-slot antenna</b>   | <b>52</b> |
| <b>5.3. PEC backed rectangular-slot antenna</b>   | <b>54</b> |
| <b>5.4. Comparison of the performance of the slot antenna</b>                                     | <b>57</b> |
| <b>5.5. Antenna Radiation Pattern Results and Discussion</b>                                      | <b>58</b> |
| <b>CONCLUSION</b>   | <b>60</b> |
| <b>FUTURE SCOPE</b>   | <b>62</b> |
| <b>REFERENCES</b>   | <b>63</b> |

# 1. INTRODUCTION

---

---

## 1.1. Electromagnetic Band Gap Structures

In recent years a class of periodically loaded structures, commonly referred to as electromagnetic band-gap (EBG) structures have been employed in a wide variety of electromagnetic devices including compact waveguides and surface wave band-gap structures. These Electromagnetic band gap (EBG) [1] materials provide frequency bands (so-called band gaps or stop bands) in which waves cannot propagate in the materials.

Any electromagnetic disturbance that is excited in such a structure will not propagate if its frequency constituents lie within the stop band of the EBG structure. These EBG materials are creating new possibilities for controlling and manipulating the flow of electromagnetic waves. Within the EBG material, there is a range of frequencies where propagating modes can be fully suppressed. This range of frequencies is known as the EBG.

EBG materials can provide significant advantages for suppressing and directing radiation when used in antennas. Many novel antennas based on EBG technology are already finding useful applications. EBG substrates are used for reducing surface waves and increasing radiation efficiency or to lower the profile of antenna design.

EBG structures have been integrated with patch antennas for enhanced performance due to the band gap of surface-wave suppression [2]. They have also been used as ground planes of spiral [3] and curl antennas [4] to achieve low profile designs.

The stop band of the EBG structures has also been applied to suppress leakage of guided-wave structures, including conductor-backed coplanar waveguides (CB CPW's) [5] and striplines [6]. Furthermore, EBG structures can realize a magnetic surface at the stop band frequency when using it as a planar reflector [7]. This property of EBG structures of realizing a magnetic surface at the stop band frequency has been used in the waveguide walls [8] to provide magnetic boundary conditions. A relatively uniform field distribution along the cross section of the waveguide has been measured. Thus these EBG structures find a wide range of applications in various electromagnetic devices.

## 1.2. Need for Electromagnetic Band Gap Structures

As we know that, a flat metal sheet is used in many antennas as a reflector, or ground plane. The presence of a ground plane redirects half of the radiation into the opposite direction, improving the antenna gain by 3dB and partially shielding objects on the other side. But it has the unfortunate property of reversing the phase of reflected waves. If the antenna is too close to the conductive surface, the phase of the impinging wave is reversed upon reflection, resulting in destructive interference with the wave emitted in the other direction. This is equivalent to saying that the image currents in the conductive sheet cancel the currents in the antenna, resulting in poor radiation efficiency. Fig. 1.1 depicts an antenna in close proximity with a flat, conducting slab. The antenna is effectively shorted out by the metal surface and negligible radiation is emitted.

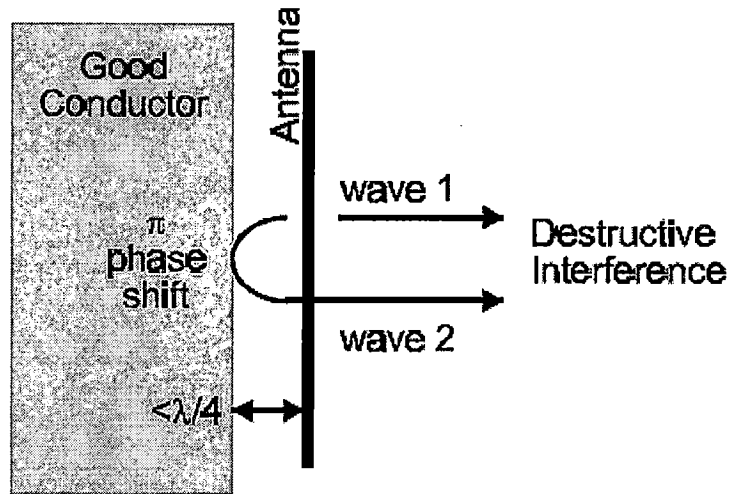


Fig. 1.1. An antenna lying flat against a ground plane

This problem is solved by including a one-quarter wavelength space between the radiating element and the ground plane, as shown in Fig. 1.2. The total round trip phase shift from the antenna, to the surface and back to the antenna, equals one complete cycle and the waves add constructively. The antenna radiates efficiently, but the entire structure requires a minimum thickness of  $\lambda/4$ . This makes the overall profile large which is not desired in many applications.

The solution to this problem can be done by using EBG structure as our ground plane and utilizing its in phase reflection characteristics, we can obtain a low profile geometry which will be helpful to various microstrip antennas application. We will be discussing this property of EBG surfaces in detail in second chapter.



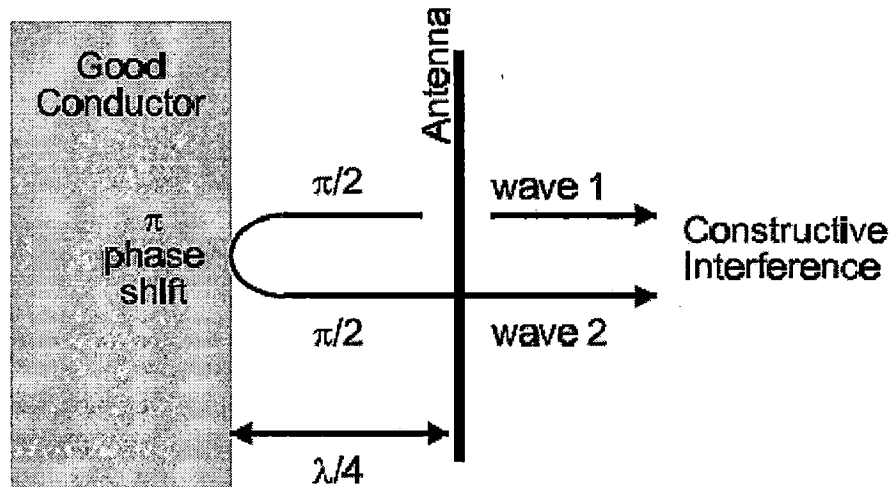
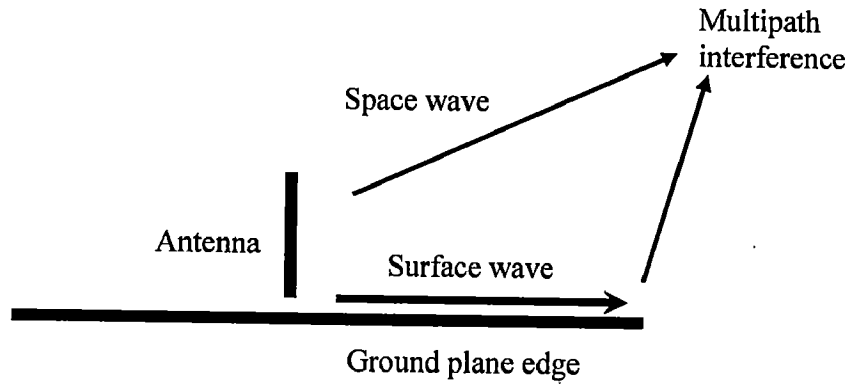


Fig. 1.2. An antenna separated by  $\lambda/4$  wavelength from the ground plane

Another property of metals is that they support surface waves. These are propagating electromagnetic waves that are bound to the interface between metal and free space. They are nothing more than the normal AC currents that occur on any electric conductor. If the conductor is smooth and flat, the surface waves will not couple to external plane waves. However, they will radiate if scattered by bends, or discontinuities.

If an antenna is placed near a metal sheet, such as a reflector, it will radiate plane waves into free space, but it will also generate surface waves that propagate along the sheet. On an infinitely large ground plane, the surface waves would be evident only as a slight reduction in radiation efficiency. In reality, the ground plane is always finite in size and these waves propagate until they reach an edge or corner. Any break in the continuous translational symmetry of the smooth, flat surface allows the waves to radiate. The result is a kind of multipath interference, illustrated in Fig. 1.3, which can be seen as ripples in the far field radiation pattern. Moreover, if multiple antennas share the same ground plane, surface currents can cause unwanted mutual coupling between them.

As we also know that if we want our antenna to be compact in size, we can achieve it by designing our circuit on high dielectric-constant substrates, which has an effect of reducing the bandwidth that can be increased by increasing substrate thickness. However, using thick substrates greatly decreases antenna efficiency due to significant surface-wave losses.



**Fig. 1.3. Multipath interference due to surface waves on a ground plane**

The problem of surface waves can be alleviated by loading the high permittivity substrate with so-called electromagnetic band gap structure (EBG) and operating the EBG structure in its forbidden frequency range where surface wave cannot propagate. Since surface waves cannot propagate along the substrate, an increased amount of radiated power couples to space waves and this mechanism has the effect of reshaping the antenna pattern. Thus, the EBG structure has the possibility of integrating antennas on high dielectric constant substrates without losing performance.

The problem of mutual coupling in array applications can also be solved by inserting the EBG structure in between the array elements and utilizing its property of surface-wave suppression, so that we can greatly reduce the unwanted mutual coupling between array elements and interference with on-board systems.

In this work, we aim to develop an Electromagnetic Band Gap structure for application in various printed antennas.

### **1.3. Literature survey**

Two technologies have been mainly pursued thus far, to achieve microstrip antennas on high-dielectric constant substrates with optimum performance. One is based on micromachining technology [9] while the other makes use of the concept of Electromagnetic band gap (EBG) substrates. In the first case, part of the substrate underneath the radiating element is removed to realize a low effective dielectric-constant environment for the antenna. In this way, power losses due to surface-wave excitation are reduced, while coupling of radiated power to space waves is enhanced. The second

alternative is to use the EBG materials as these materials provide frequency bands (so called stop band or band gap) inside which waves cannot propagate. Therefore, surface waves will not be allowed to propagate along the substrate and, hence, an increased amount of radiated power couples to space waves and this mechanism has the effect of reshaping the antenna pattern.

Several configurations have been proposed in the literature to realize EBG substrates. The first attempts were made by drilling a periodic pattern of holes in the substrate [2] as shown in Fig. 1.4 or by etching a periodic pattern of circles in the ground plane [10],[11].

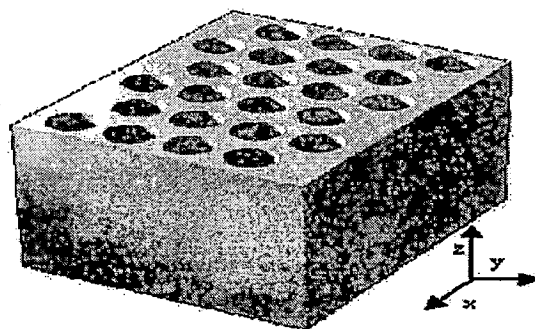


Fig. 1.4. Three dimensional view of the EBG surface formed by embedding air columns in a dielectric substrate [2]

A woodpile EBG was investigated in [12], as a periodic structure capable of producing complete transmission band-gap regions as shown in Fig. 1.5. In the design presented in [12], only dielectric materials were used to obtain the band-gap structure and the wave impedance contrast exists between the layers ( $\eta_2/\eta_1 = \sqrt{[\epsilon_o/\epsilon_e]}$ ) that is responsible for the rejection level at the band-gap region.

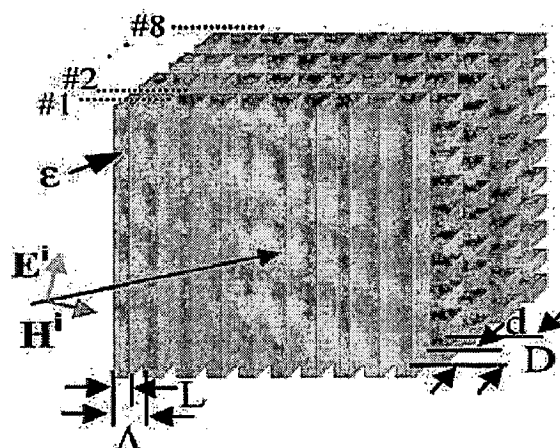
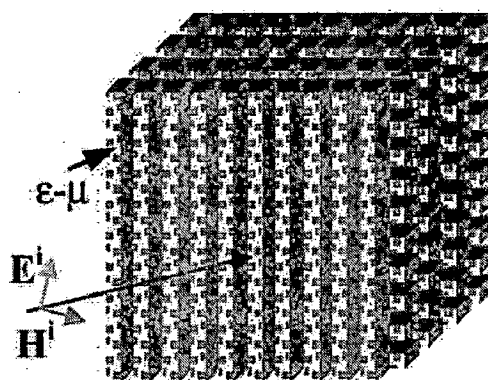


Fig. 1.5. Eight layer Dielectric Woodpile EBG structure ( $\epsilon$  material) [13]

In [13], a woodpile structure composed of magneto-dielectric material was considered which shows superior band-gap characteristics which is shown in Fig. 1.6. It was shown that the magneto-dielectric woodpile not only exhibits band-gap rejection values much higher than the ordinary dielectric woodpile, but also for the same physical dimensions, it shows a rejection band at a much lower frequency. The higher rejection is a result of higher effective impedance contrast between consecutive layers of the magneto-dielectric woodpile structure ( $\eta_2/\eta_1 = \sqrt{[(\mu_o/\epsilon_e).(\epsilon_o/\mu_e)]}$ ). This is because here both the permittivity and permeability are increasing the mismatch while in case of dielectric woodpile only permittivity was responsible for the mismatch. These Magneto-dielectrics are also shown to provide certain advantages when used as substrates for planar antennas. These substrates are used to miniaturize antennas while maintaining a relatively high bandwidth and efficiency. A resonator antenna made from a dielectric woodpile electromagnetic band gap is described in [1], to obtain a highly directive radiation pattern and at the same time, the antenna has the advantages of low height, low loss and low side lobes.



**Fig. 1.6. Eight layer Magneto-Dielectric Woodpile EBG structure ( $\epsilon$ - $\mu$  material) [13]**

A more effective and compact approach, which makes use of a triangular or square lattice of metallic pads connected to ground with vias, has been recently proposed by Sievenpiper [14] and applied in [15] to enhance the gain of a planar antenna as shown in Fig. 1.7. The structures presented in [14] are the first realizations of planar compact electromagnetic crystal with a complete stop band in the microwave range.

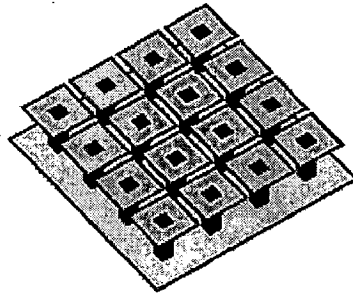


**Fig. 1.7. Mushroom like EBG structure [14]**

Subsequent research efforts have led to the realization of a uniplanar compact Photonic band gap (UC-PBG) substrate [16] (Fig. 1.8) whose applications to planar slow-wave structures and low-leakage conductor-backed coplanar waveguide have been recently presented [16], [18].

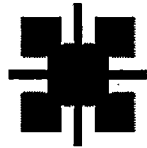


**Fig. 1.8. Layout of the UC-PBG unit cell [16]**

Advantageous features of this crystal substrate include simple low-cost manufacturing (no vias are necessary) and compatibility with standard monolithic microwave integrated circuits (MMIC's) fabrication technology. In 1999, R. Coccioli, F. R. Yang, K. P. Ma and T. Itoh [19] used the uniplanar compact Electromagnetic band gap (UC-EBG) substrate successfully to reduce surface-wave losses for an aperture-coupled fed patch antenna on a thick high dielectric-constant substrate. In [20], EBG surfaces are designed to act as an AMC ground plane over a desired narrow frequency range, moreover, several different design methodologies for multiband artificial magnetic conducting (AMC) surfaces has been introduced.

Other favorable effects brought by surface-wave suppression are the reduction of unwanted mutual coupling between array elements and interference with on-board systems. In 2003, Y. Rahmat-Samii and F. Yang [21] analyzed a mushroom-like EBG structure and demonstrated its band-gap feature of surface-wave suppression by exhibiting the near field distributions of the electromagnetic waves. They inserted an EBG structure between array elements to reduce the mutual coupling. As a result, a significant amount of reduction in mutual coupling was noticed.

The band-gap features of EBG structures can be revealed in two ways: the suppression of surface-wave propagation and the in-phase reflection coefficient. The feature of surface-wave suppression helps to improve antenna's performance such as increasing the antenna gain and reducing back radiation [19], [21]. The in-phase reflection feature leads to low profile antenna designs [22]-[24]. When plane waves normally illuminate an EBG surface, the phase of the reflected field changes continuously from  $180^\circ$  to  $-180^\circ$  with frequency. It has been shown in [22]-[24] that one can replace a conventional perfect electric conductor (PEC) ground plane with an EBG ground plane for a low profile wire antenna design.

In [25], a compact and very low profile spiral curl antenna was designed using a small EBG ground plane, to obtain a good circular polarization, with an overall height less than 2.5% of wavelength.

Various applications of the mushroom-like EBG structure were shown in [26] that include the design of low profile circularly polarized curl antennas and its capability in suppressing the surface wave in microstrip antennas. In 2003, M. Fallah-Rad and I. Shafai [27], showed a significant amount of improvement in the gain and radiation pattern by using a single layer of EBG around a patch antenna. In addition to this, it was also shown that the back radiation due to the finite ground plane reduces significantly.

In [28], the same author proposed a more simplified form of EBG structure and studied its effect on the impedance bandwidth, gain and cross-polarization level performance on an aperture-coupled rectangular microstrip antenna.

In [29] and [30] a fork-like shaped electromagnetic-band gap (EBG) structure has been investigated and a comparison has been carried out between this structure and the conventional mushroom-like EBG structure, showing that the fork-like structure has an extremely compact size.

In [31], a uni-directional ring slot antenna was achieved by backing them with an electromagnetic band-gap surface, instead of the uniform conducting reflector, as using the electromagnetic band-gap surface makes the overall antenna of low profile. At the same time, it reduces the parallel-plate mode which was generated in case of conducting reflector resulting in an increase in the radiation efficiency.

#### 1.4. Motivation and Scope

With the requirements of compact and high efficient antennas for modern applications, the general method that is being used is to build the printed antennas on high dielectric constant substrates which results in lower bandwidth. For increasing the bandwidth, we generally increase the height of the antenna which increases the surface wave problem and hence results in lower radiation efficiency.

By using an EBG structure in the antenna architecture and utilizing its property of reducing surface waves, we can reduce size, weight and losses of the antennas. In this dissertation, the design of a new EBG structure is being proposed which is shown in Fig. 1.9. The structure is a modification of a mushroom type structure. This proposed structure provides more bandwidth because of two different resonant lengths in two directions. Also this structure is more compact in the sense that its elements are closely interlocked with each other.

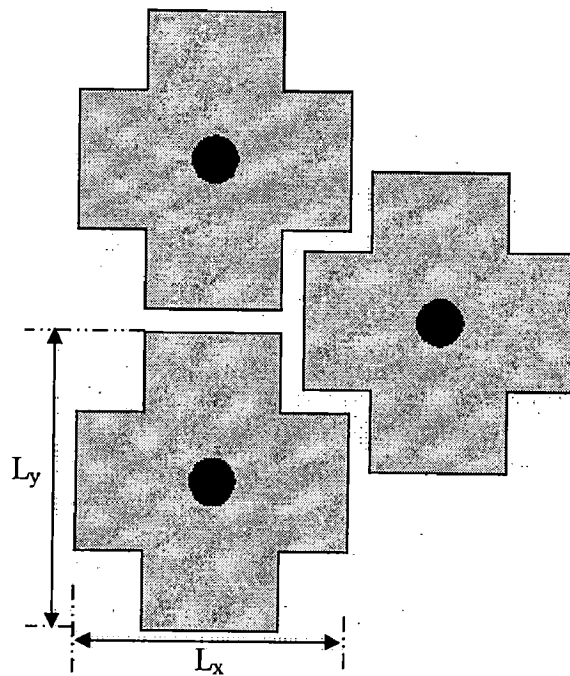


Fig. 1.9. Three elements of the proposed EBG structure

## 1.5. Problem Statement

- (a) Design optimization of an Electromagnetic Band Gap structure at 5 GHz and to find out the band gap of the proposed EBG structure.
- (b) To study mutual coupling effects between array elements without EBG isolation and with EBG isolation.
- (c) Effect of the proposed EBG surface on the radiation characteristics of a dipole antenna.
- (d) Effect of the proposed EBG surface on the radiation characteristics of a microstrip slot antenna.

## 1.6. Organization of the Dissertation

This thesis focuses on the development of a new EBG structure and its application to printed antennas and arrays. The total work is organized in five chapters.

As has been seen the first chapter introduces the Electromagnetic band gap structures and briefly discusses their properties, their benefits and applications. This chapter also presents a discussion about the work that has already been carried out by researchers in the Electromagnetic band gap community in recent years.

In second chapter, the design and parametric study of the EBG surface proposed in this study is presented. Its working principle and its equivalent lumped circuit element is also described there.

In third chapter, the mutual coupling of microstrip antennas are parametrically investigated, for both the E-plane and H-plane coupling directions, for different substrate thickness and for various dielectric constants. A reduction in mutual coupling using EBG structure between array elements is also shown.

The fourth chapter focusses on the reflection phase feature of EBG surfaces; when plane waves normally illuminate an EBG structure, the phase of the reflected field changes continuously from  $180^\circ$  to  $-180^\circ$  versus frequency. As we know that dipole antennas do not function effectively when positioned very closely and parallel above a PEC (perfect electric conductor) ground plane due to the reverse image currents, which reduce the radiation efficiency. This chapter shows the use of EBG structure as a ground plane for



wire antenna design to reduce the geometric profile as compared to the case when PEC is used as a ground plane.

The fifth chapter deals with slot antennas where main drawback is that they are inherently bi-directional radiators. One common technique to redirect the back radiation forward is to place a conducting reflector at a fixed distance away from the antenna. This, however increases the size of the antenna structure and, also, reduces the radiation efficiency. This chapter describes a solution to this problem and shows how to achieve uni-directional slot antenna elements by backing them with an electromagnetic band-gap surface, instead of the uniform conducting reflector.

Finally, the last chapter of this dissertation gives the concluding remarks and the future scope of the proposed EBG structure.

## 2. DESIGN AND PARAMETRIC STUDY OF THE PROPOSED EBG STRUCTURE

---

---

By incorporating a special texture on a conductor, it is possible to alter its radio frequency surface properties. In the limit, where the period of the surface texture is much smaller than the wavelength, the qualities of the structure can be summarized into a single parameter, the surface impedance. This boundary condition defines the ratio of the tangential electric field to the tangential magnetic field at the surface. In this chapter, we first discuss the physics behind the EBG surfaces and then propose and study a new EBG structure.

### 2.1. Working Principle of EBG structure

A cross section of a typical EBG structure is shown in Fig. 2.1. This EBG surface consists of 4 parts, the bottom metal ground plane, the dielectric substrate, the top periodic patch lattices and the vias inside the dielectric substrate which connect the bottom ground plane and the top lattices.

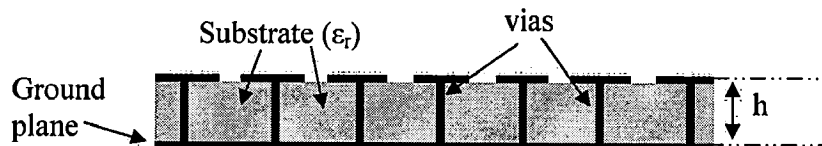
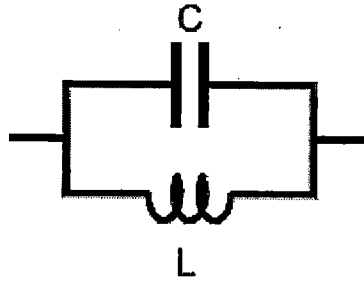


Fig. 2.1. Cross-section of an Electromagnetic Band Gap surface

Since the patch lattice is small compared to the wavelength, the electromagnetic properties can be described using lumped circuit elements -capacitors and inductors. The gap between neighboring patch lattice provides the capacitance and the conducting path of vias, which connect the bottom plane and the top patch lattice, provides the inductance. Together, they behave as parallel resonant LC circuits. The capacitance  $C$  in this LC model actually comes from the fringing electric field between adjacent metal patch lattices and the inductance originates from current loops within the structure. The electromagnetic properties of the surface can be reduced to an equivalent LC circuit, shown in Fig. 2.2.



**Fig. 2.2. Equivalent circuit model for the high-impedance surface**

The impedance of a parallel resonant LC circuit is given by,

$$Z = \frac{j\omega L}{1 - \omega^2 LC} \quad (1)$$

It is inductive at low frequencies and capacitive at high frequencies. In a narrow band around the LC resonance, the impedance is very high. In this frequency range, currents on the surface radiate very efficiently and the structure suppresses the propagation of surface waves. Thus over a certain frequency range, this structure shows Electromagnetic band gap property.

This Electromagnetic band gap surface acts as a high impedance surface at resonant frequency. The impedance crosses through infinity at the resonance frequency which is given by

$$\omega_o = \frac{1}{\sqrt{LC}} \quad (2)$$

In the frequency range where the surface impedance is very high, the tangential magnetic field is small, even with a large electric field. Such a structure is sometimes described as a “magnetic conductor”. This is a mathematical idea that is used in certain electromagnetic problems, but does not exist in reality. Thus over a certain frequency range where this EBG structure has high impedance, it can be regarded as a kind of magnetic conductor.

Because of this unusual boundary condition, the high-impedance surface can function as a unique new type of ground plane for low-profile antennas. For example, a simple dipole lying flat against a high-impedance ground plane, shown in Fig. 2.3, is not shorted out as it would be on an ordinary metal ground plane. The high-impedance surface reflects all of the power just like a metal sheet, but it reflects in-phase, rather than out-of-phase, allowing the radiating element to be directly adjacent to the surface. In other words, the

direction of the image currents results in constructive, rather than destructive interference, allowing the antenna to radiate efficiently. Furthermore, in a forbidden frequency band, the high-impedance ground plane does not support freely propagating surface currents, resulting in an improved radiation pattern.

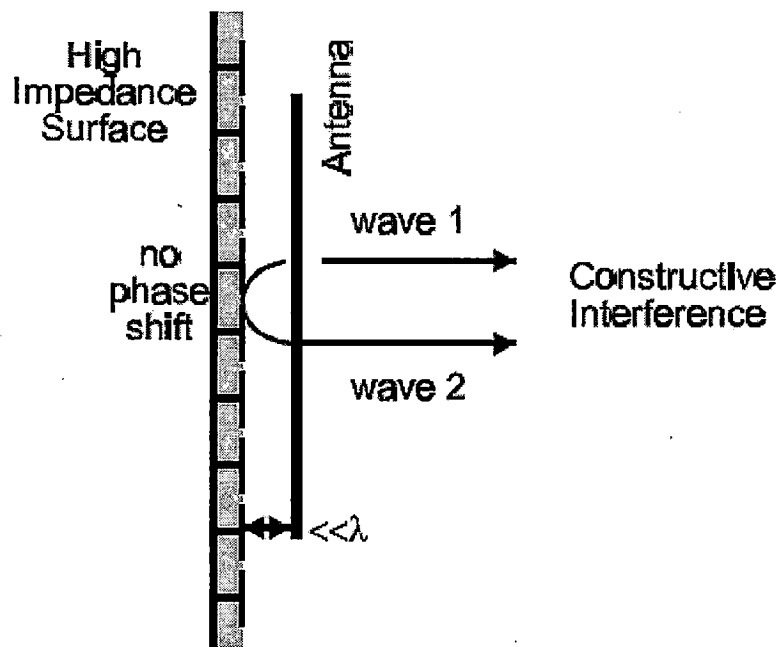


Fig. 2.3. Dipole on a high-impedance ground plane

Thus from the above discussion we can point out the two unusual electro-magnetic properties that Electromagnetic Band Gap structures exhibits:

- 1) It does not allow radio frequency electric currents to propagate along the surface, i.e. it is an RF open, while being a dc short.
- 2) It reflects electromagnetic radiation in-phase, rather than out-of-phase as a normal metal surface does.

## 2.2. A Corrugated Surface approach to EBG

The Electromagnetic Band gap structures can also be understood by examining a similar structure, the corrugated surface. Corrugated surface is a metal slab, into which a series of vertical slots have been cut, as depicted in Fig. 2.4. The slots are narrow, so that many of them fit within one wavelength across the slab. Each slot can be regarded as a parallel-plate transmission line, running down into the slab and shorted at the bottom. If the slots are one-quarter wavelength deep, then the short circuit at the bottom end is transformed

by the length of the slot into an open-circuit at the top end and the impedance at the top surface is very high.

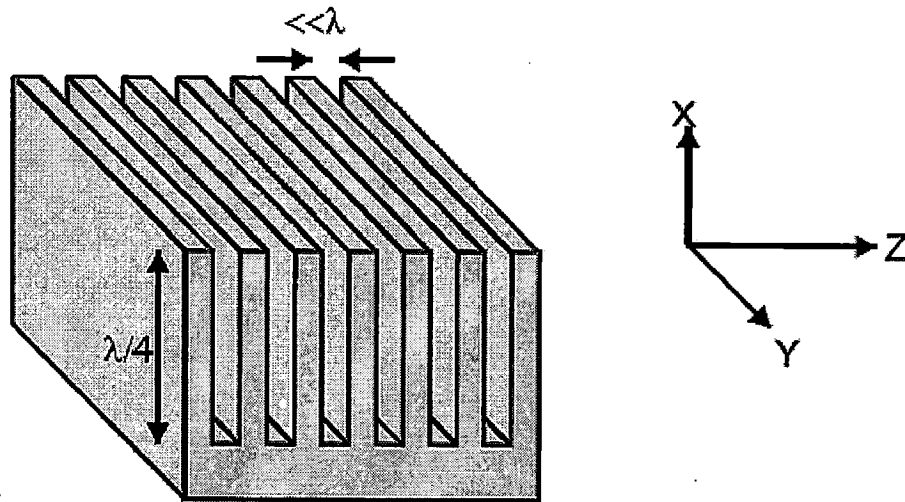


Fig. 2.4. A corrugated metal slab

Thus the property of the EBG structures is similar to those of the corrugated slab. The quarter-wavelength slots have simply been folded up into lumped elements – capacitors and inductors – and distributed in two dimensions as shown in Fig. 2.5.

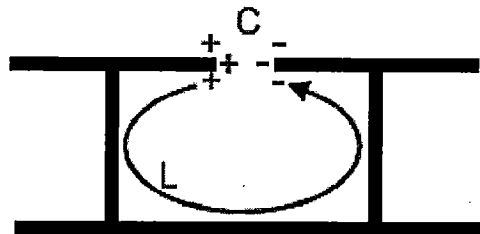


Fig. 2.5. Origin of the equivalent circuit elements

The resonance frequency is solely determined by the geometric and material parameters of the structure. The relevant parameters are the slot gap widths and the radius and height of the vias along with the permittivity and permeability of the substrate. This two layer structure may be thought of as a modified ground plane.

### 2.3. Proposed EBG structure

The three dimensional view of the EBG structure that is being proposed in this work is shown in Fig. 2.6. The top view is shown in Fig. 2.7. This EBG structure consists of 4 parts: the bottom metal ground plane, the dielectric substrate, the top periodic patch lattices and the vias inside the dielectric substrate which connect the bottom ground plane and the top lattices.

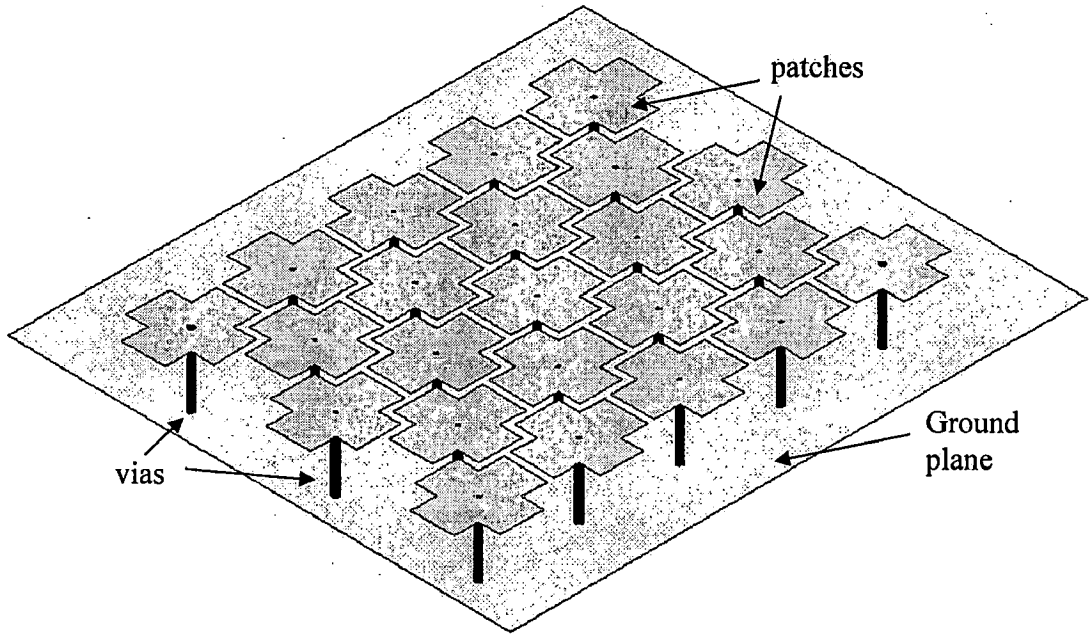


Fig. 2.6. Three dimensional view of the proposed EBG structure

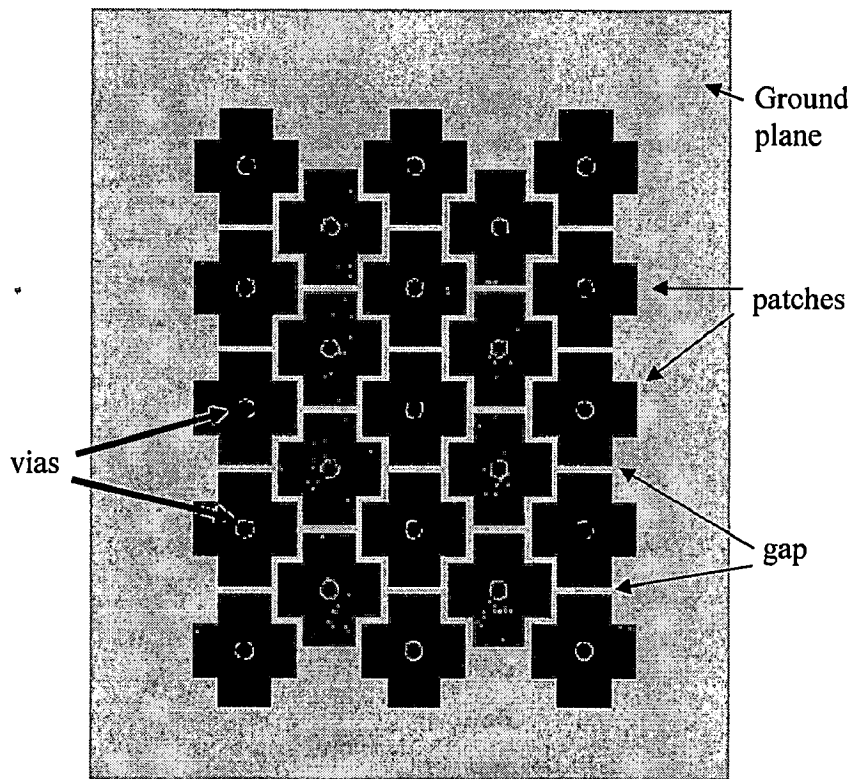


Fig. 2.7. Top view of the EBG surface

## 2.4. Parametric study of the EBG surface

Parametric studies have been performed to obtain design guidelines for EBG ground planes. The band gap of the proposed EBG surface is mainly determined by the following parameters: patch width along x axis ( $L_x$ ), patch width along y axis ( $L_y$ ), gap width ( $g$ ), substrate permittivity ( $\epsilon_r$ ) and substrate thickness ( $h$ ), as can be seen in Fig. 2.8 and Fig. 2.9. In this section, the effects of these parameters are discussed one by one using simulation on IE3D simulation software. Transmission coefficient ( $S_{21}$ ) is being measured between the two reference planes P1 and P2 to find out the band gap of the proposed EBG surface.

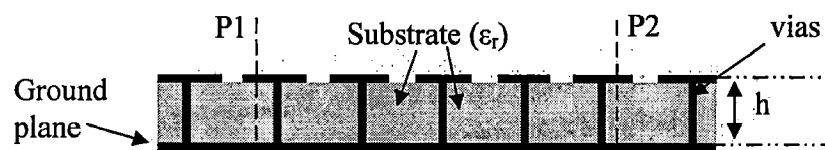


Fig. 2.8. Side view of a single layer EBG surface

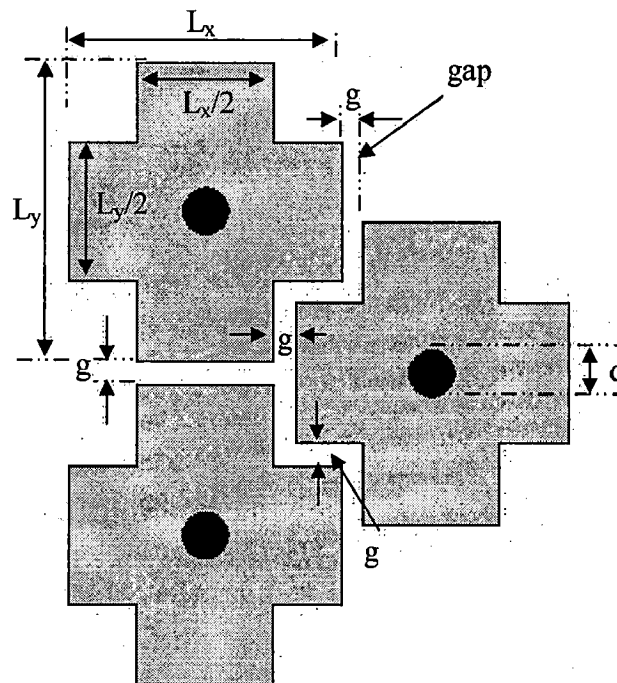


Fig. 2.9. Three elements of EBG structure

### a. Patch Width Effect

Patch width plays an important role in determining the frequency band. To study the effect of the EBG patch width, other parameters such as the gap width, via diameter,

substrate permittivity and substrate thickness are kept as:  $\epsilon_r=10.5$ ,  $h=1.27\text{mm}$ , while we change the patch width.

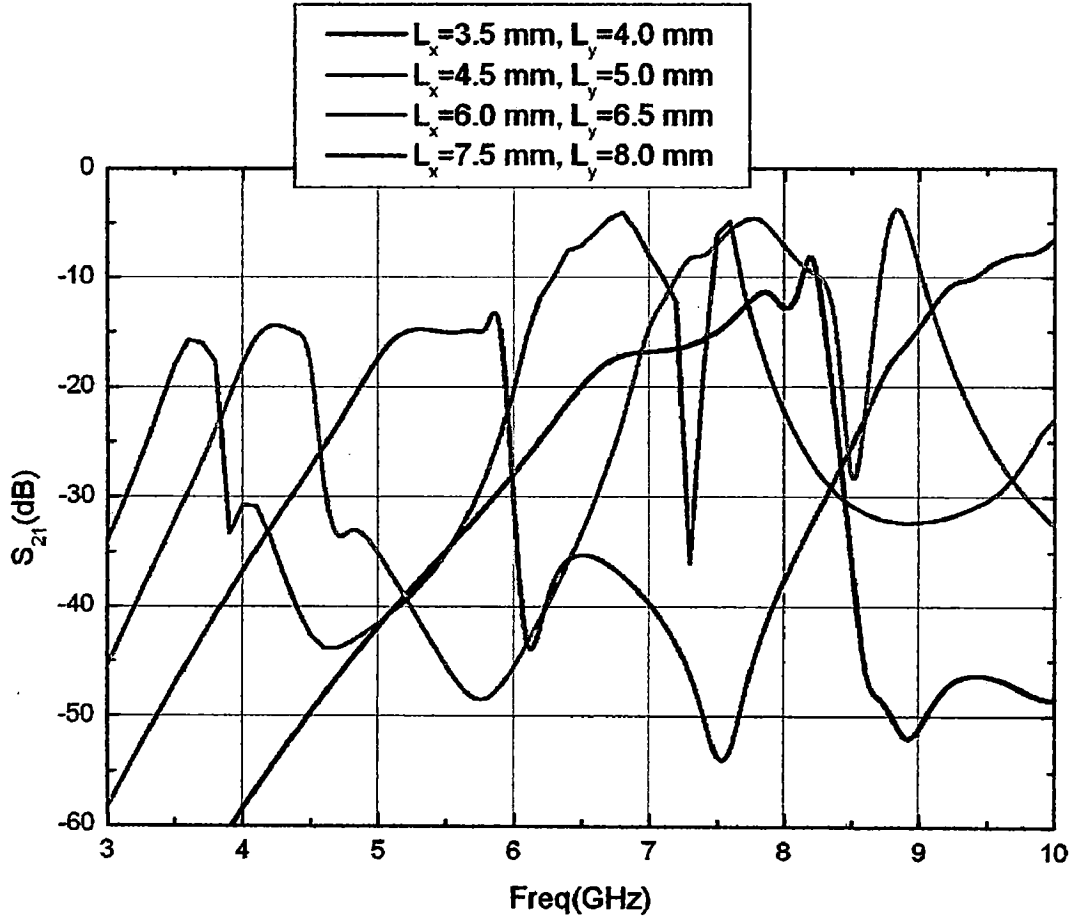


Fig. 2.10. Band gap of the EBG structure versus patch width

Fig. 2.10 shows the transmission coefficient ( $S_{21}$ ) versus frequency between the two reference planes of the EBG surface with different patch widths. In this work, the band gap has been defined to be the frequency band for which  $S_{21}$  is less than -30 dB. It can be observed from Table 2.1 that when the patch size is increased, the frequency band shifts downward and the band gap decreases.

Table 2.1. Band gap versus patch width

| Patch Width                          | Frequency Range | Band Gap |
|--------------------------------------|-----------------|----------|
| $L_x=3.5\text{mm}, L_y=4.0\text{mm}$ | 8.44-11.21 GHz  | 2.77 GHz |
| $L_x=4.5\text{mm}, L_y=5.0\text{mm}$ | 5.99-8.30 GHz   | 2.31 GHz |
| $L_x=6.0\text{mm}, L_y=6.5\text{mm}$ | 4.59-6.60 GHz   | 2.01 GHz |
| $L_x=7.5\text{mm}, L_y=8.0\text{mm}$ | 3.87-5.72 GHz   | 1.84 GHz |



*b. Gap Width Effect*

The gap width is the distance between adjacent patches. It controls the coupling of EBG patch units. Variation of the gap width affects the frequency band of the EBG surface. During this investigation, the patch width, via diameter, substrate permittivity and substrate thickness are kept the same as:  $L_x=6.0\text{mm}$ ,  $L_y=6.5\text{mm}$ ,  $d=0.8\text{mm}$ ,  $\epsilon_r=10.5$ ,  $h=1.27\text{mm}$ . The gap width is increased from 0.25 to 1.0mm.

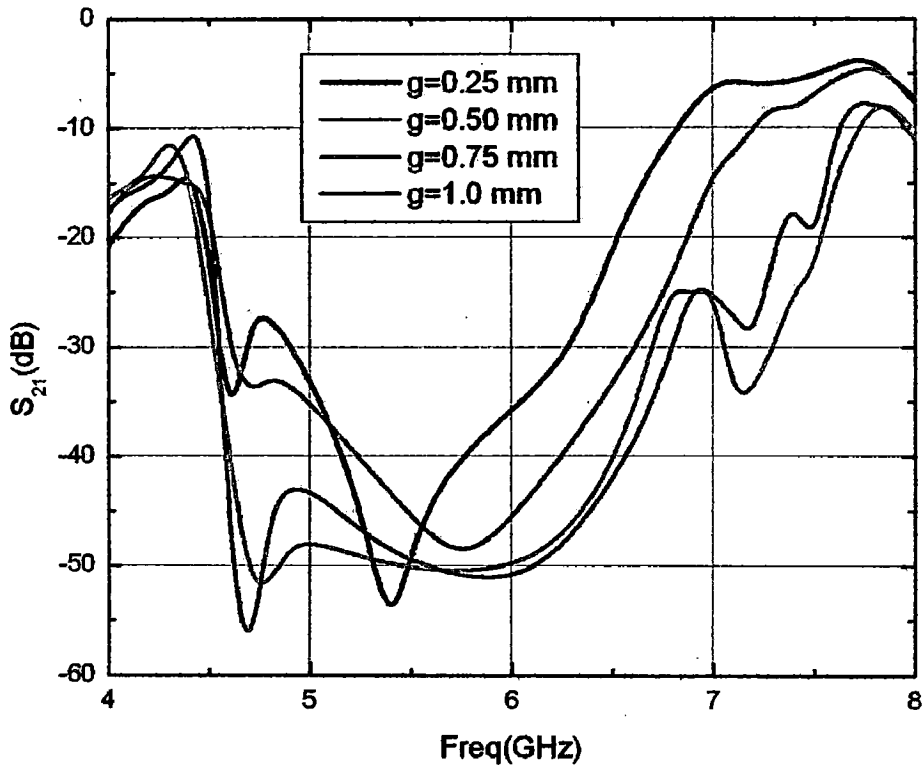


**Fig. 2.11. Band gap of the EBG structure versus gap width**

Fig. 2.11 displays the transmission coefficient ( $S_{21}$ ) versus frequency between the two reference planes for different gap widths. As can be seen from Table 2.2, as the gap width increases, band gap increases.

**Table 2.2. Band gap versus gap width**

| Gap Width           | Frequency Range | Band Gap |
|---------------------|-----------------|----------|
| $g = 0.25\text{mm}$ | 4.9-6.27 GHz    | 1.37 GHz |
| $g = 0.50\text{mm}$ | 4.6-6.59 GHz    | 1.99 GHz |
| $g = 0.75\text{mm}$ | 4.52-6.71 GHz   | 2.19 GHz |
| $g = 1.0\text{mm}$  | 4.53-6.82 GHz   | 2.29 GHz |

### c. Substrate Permittivity Effect

Relative permittivity ( $\epsilon_r$ ) of the substrate is another effective parameter used to control the frequency band. During this investigation, the patch width, gap width, via diameter and substrate thickness is kept the same as:  $L_x=6.0\text{mm}$ ,  $L_y=6.5\text{mm}$ ,  $g=0.5\text{mm}$ ,  $d=0.8\text{mm}$ ,  $h=1.27\text{mm}$  while its permittivity is changed from 4 to 10.

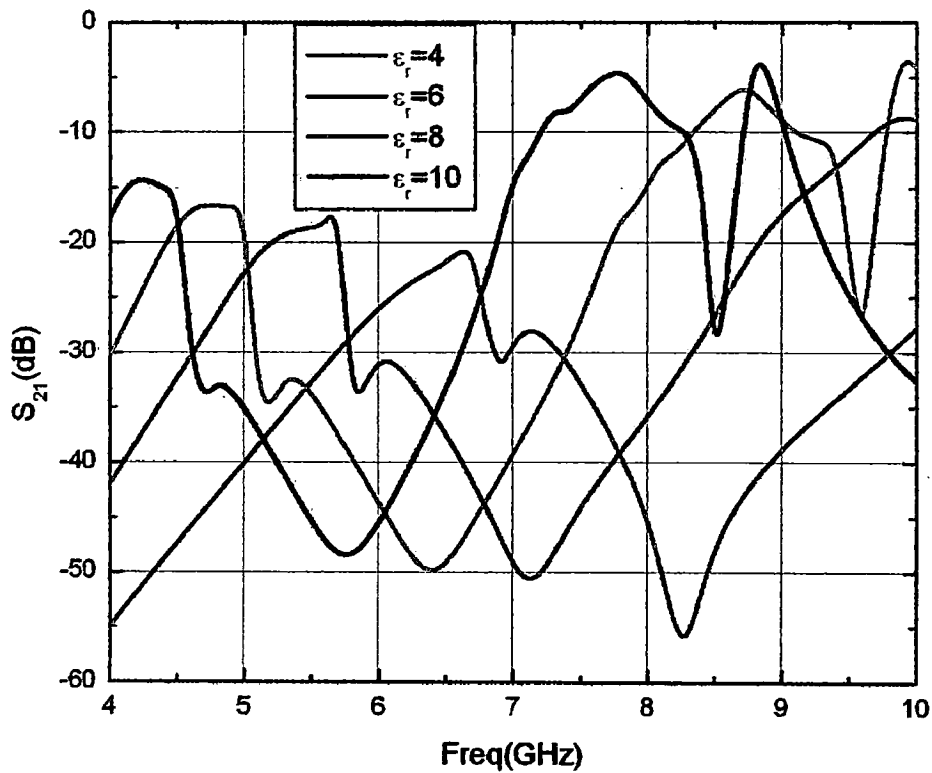


Fig. 2.12. Band gap of the EBG structure versus substrate permittivity

The transmission coefficient ( $S_{21}$ ) versus frequency between the two reference planes for various permittivities is plotted in Fig. 2.12. It can be observed from Table 2.3 that as substrate permittivity increases band gap position shifts downward.

Table 2.3. Band gap versus substrate permittivity

| Substrate permittivity | Frequency Range | Band Gap |
|------------------------|-----------------|----------|
| $\epsilon_r = 4$       | 7.34-9.80 GHz   | 2.46 GHz |
| $\epsilon_r = 6$       | 5.77-8.33 GHz   | 2.55 GHz |
| $\epsilon_r = 8$       | 5.07-7.39 GHz   | 2.31 GHz |
| $\epsilon_r = 10$      | 4.59-6.60 GHz   | 2.01 GHz |

#### d. Substrate Thickness Effect

In the following simulations the patch width, gap width and substrate permittivity are the same as,  $L_x=6.0\text{mm}$ ,  $L_y=6.5\text{mm}$ ,  $g=0.5\text{mm}$ ,  $d=0.8\text{mm}$ ,  $\epsilon_r=10.5$ . The substrate thickness is changed from 0.9 mm to 1.5 mm.

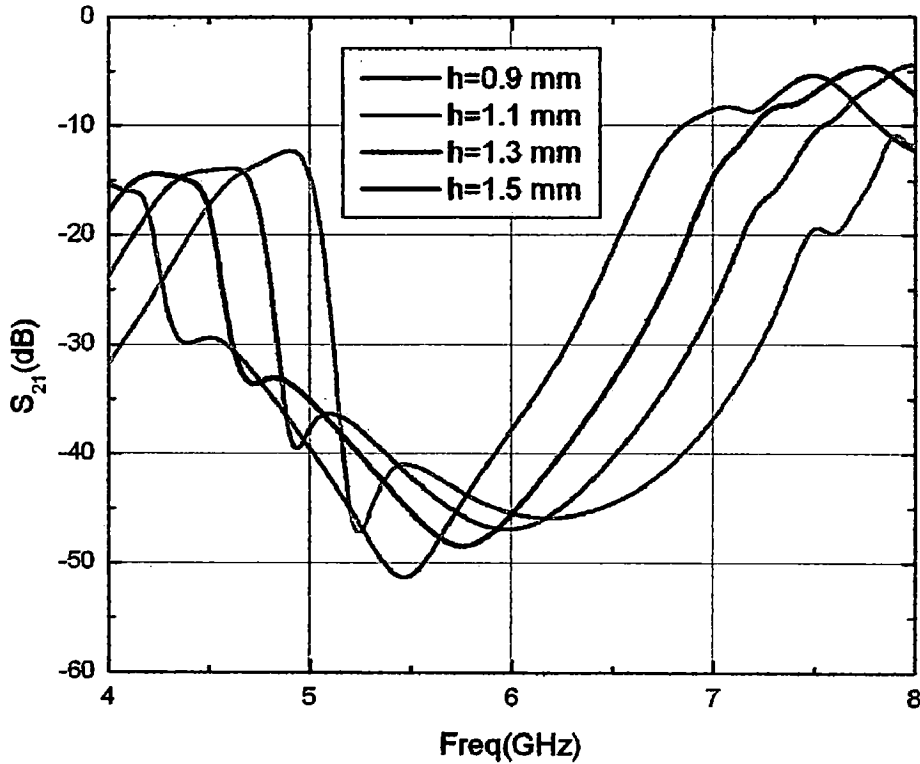


Fig. 2.13. Band gap of the EBG structure versus substrate thickness

The transmission coefficient ( $S_{21}$ ) versus frequency between the two reference planes with different substrate thicknesses is shown in Fig. 2.13. It can be observed from Table 2.4 that if the substrate thickness is increased, the band gap position shifts downward.

Table 2.4. Band gap versus substrate thickness

| Substrate thickness  | Frequency Range | Band Gap |
|----------------------|-----------------|----------|
| $h = 0.9 \text{ mm}$ | 5.12-7.23 GHz   | 2.11 GHz |
| $h = 1.1 \text{ mm}$ | 4.85-6.88 GHz   | 2.03 GHz |
| $h = 1.3 \text{ mm}$ | 4.63-6.52 GHz   | 1.89 GHz |
| $h = 1.5 \text{ mm}$ | 4.59-6.27 GHz   | 1.68 GHz |

*e. Effect of the diameter of the Vias*

The effect of the diameter of vias on the EBG surfaces properties was also investigated. The diameter of the vias was varied from 0.4 mm to 1.0 mm, keeping all other parameters as,  $L_x=6.0\text{mm}$ ,  $L_y=6.5\text{mm}$ ,  $g=0.5\text{mm}$ ,  $\epsilon_r=10.5$  and  $h=1.27\text{mm}$ . It can be observed from Table 2.5 that as diameter increases, there is a reduction in band gap as shown in Fig. 2.14.

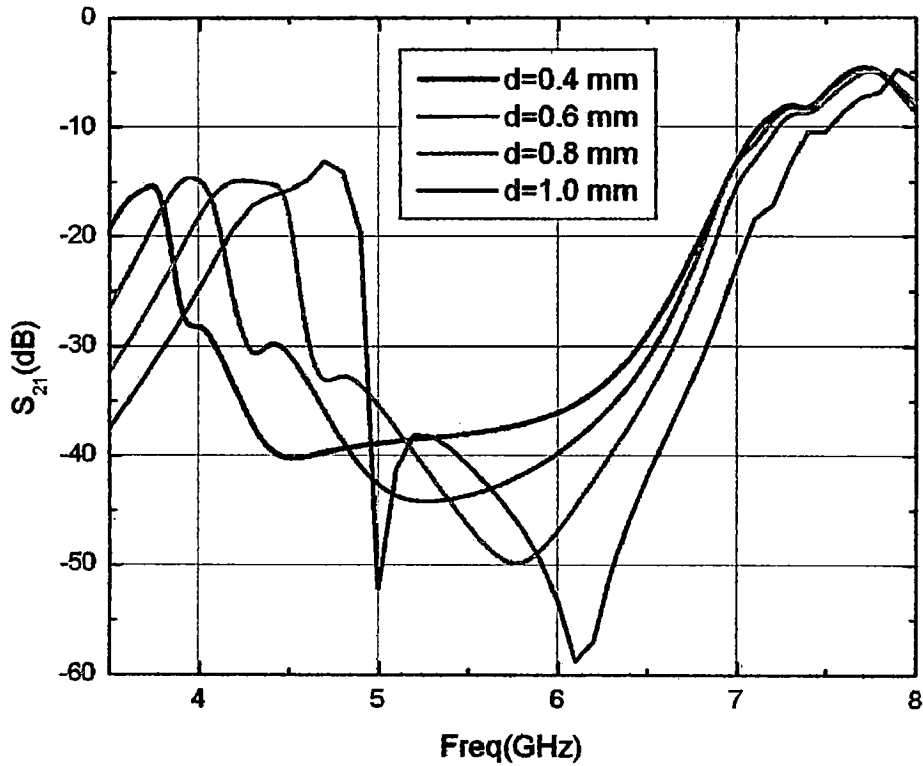


Fig. 2.14. Band gap of the EBG structure versus via diameter

Table 2.5. Band gap versus Via diameter

| Via diameter | Frequency Range | Band Gap |
|--------------|-----------------|----------|
| d = 0.4mm    | 4.09-6.45 GHz   | 2.35 GHz |
| d = 0.6mm    | 4.46-6.54 GHz   | 2.08 GHz |
| d = 0.8mm    | 4.59-6.64 GHz   | 2.04 GHz |
| d = 1.0mm    | 4.93-6.83 GHz   | 1.89 GHz |

## 2.5. Optimized Parameters of the proposed EBG structure

The optimized dimensions of the unit cell of proposed EBG structure for operation at 5 GHz are shown in Fig. 2.15. Fig. 2.16 shows the gap between the patches which is 0.5mm in all directions. A Rogers/RT duroid 6010 has been used as a substrate. The specification for this laminate is given in Table 2.6.

Table 2.6. Specification for the substrate

| Parameters                     | Values |
|--------------------------------|--------|
| $\epsilon_r$                   | 10.5   |
| Thickness                      | 1.27mm |
| Loss tangent ( $\tan \delta$ ) | 0.0023 |

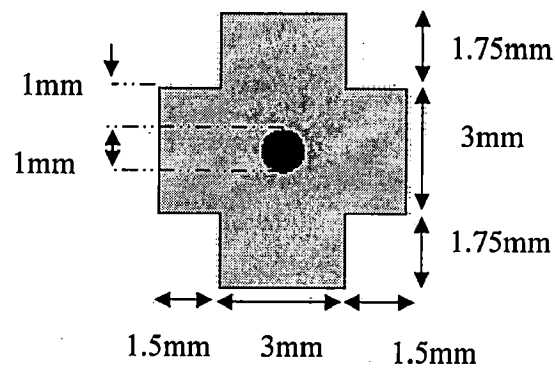


Fig. 2.15. EBG unit cell

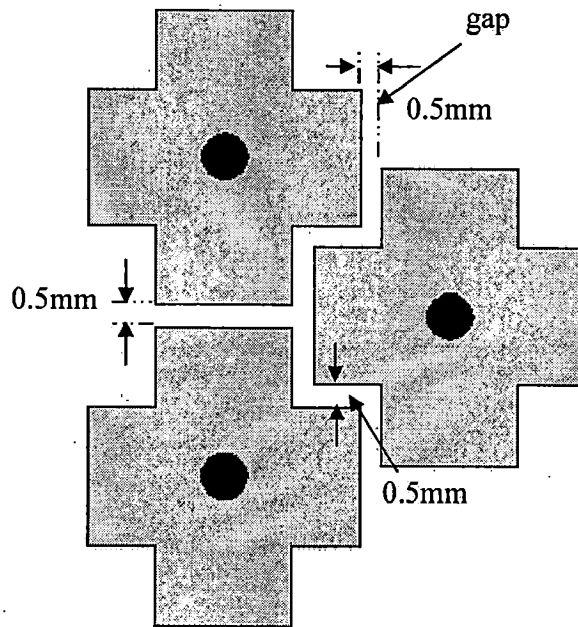


Fig. 2.16. Three elements of EBG

## 2.6. Band Gap determination method of the EBG structure

The following two methods have been investigated for the determination of the band gap of the proposed EBG structure. Also a new method is proposed for determining the band gap of the EBG structure.

- a) As has been discussed earlier, an EBG surface can be modeled as a corrugated slab. This model can be used to study the properties of the proposed EBG surface. The quarter-wavelength slots have simply been folded up into lumped elements – capacitors and inductors – and distributed in two dimensions.

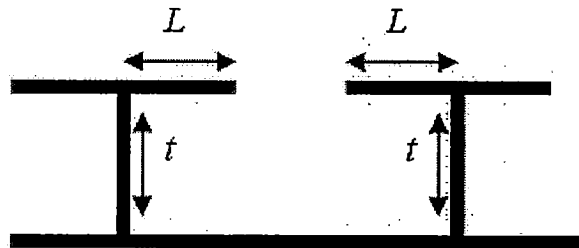


Fig. 2.17. Side view of two unit cells of EBG

Thus, the sum of  $L$  and  $t$  should be equal to  $\lambda/4$ , where  $\lambda$  is the guided wavelength. For the optimized dimension of the proposed geometry, the patch width is 6mm along X

axis and 6.5mm along Y axis. So, L should be equal to 3mm or 3.25mm (half of patch width) and the thickness of the substrate on which EBG has been designed is 1.27mm with  $\epsilon_r = 10.5$ . Therefore,

$$L = 3 \text{ or } 3.25 \text{ mm and } t = 1.27\text{mm.}$$

$$\text{Sum of L and t is } L + t = 4.27 \text{ or } 4.52\text{mm}$$

This implies  $\lambda_g/4 = 4.27 \text{ or } 4.52 \text{ mm}$  and hence,  $\lambda_g = 17.08 \text{ or } 18.08\text{mm}$ ,

Therefore, free space wavelength  $\lambda = \lambda_g \sqrt{10.5} = 55.34 \text{ or } 58.58\text{mm}$

Thus, the theoretical calculated resonant frequency comes out to be 5.42 GHz or 5.12 GHz around which the structure should exhibit a stop band.

b) In second method, the simulated environment for the band gap determination of EBG structures is shown in Fig. 2.18 [31] and this has been simulated on IE3D simulation software. An EBG array of 3 x 5 elements has been used for the determination of band gap as shown in Fig. 2.19. This EBG array consists of 3 rows and five columns of EBG with 3 elements of EBG in first column, 2 elements in second column, 3 elements in third column, 2 elements in fourth column and 3 elements in the fifth column as shown in Fig. 2.19. This pattern is being represented as [32323] henceforth. As shown, two holes are drilled into the top conductor so that co-axial probes may be placed about 27.55 mm apart along one of the main directions of periodicity. Two holes are also drilled into the slotted part of the EBG surface so that long co-axial probes may be used to detect the transmission coefficient. The outer conductor of the co-axial probe is connected to the ground plane of the top substrate and the inner conductor goes through the EBG surface and is connected to the solid ground plane of the EBG surface. From this arrangement the transmission parameter  $S_{21}$  can be measured. It is seen from the simulated results that the stop band lies from 4.5 to 5.7 GHz, (according to -30 dB criteria). The frequency where the stop band begins is seen to be very close to the value determined by the corrugated model which was at 5.12 GHz of 5.42 GHz.

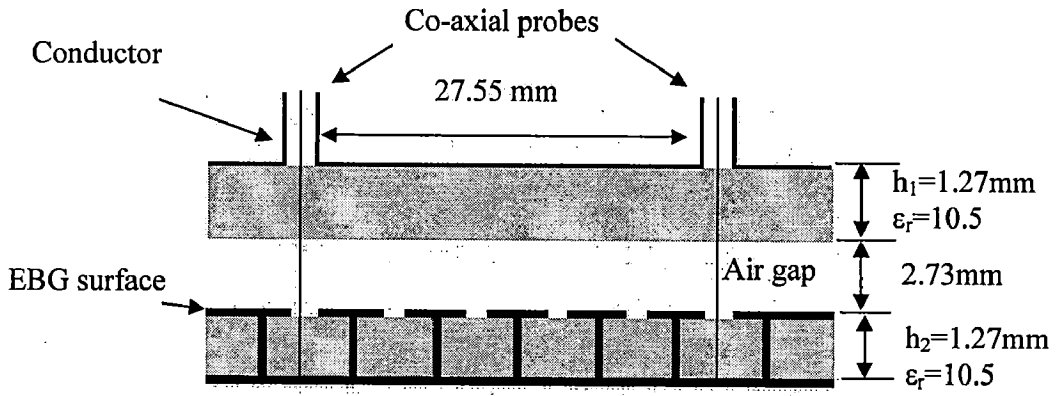


Fig. 2.18. Simulation profile for Band gap tuning in EBG structures

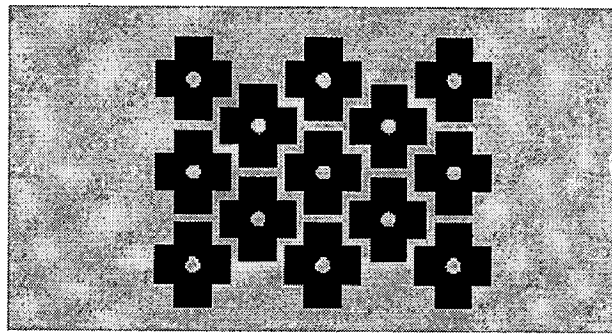


Fig. 2.19. EBG Configuration used for finding the Band Gap

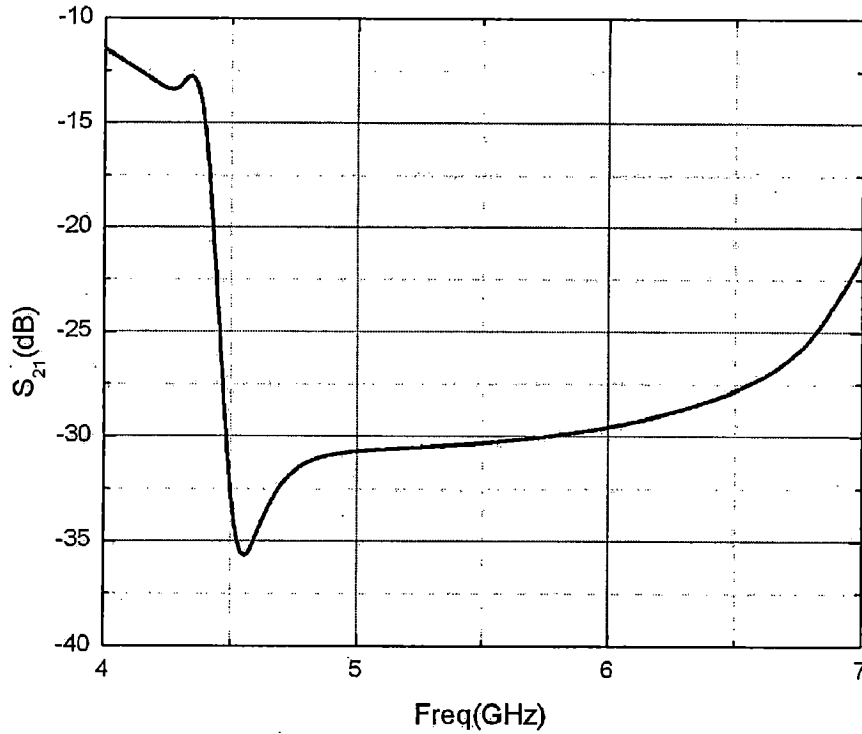
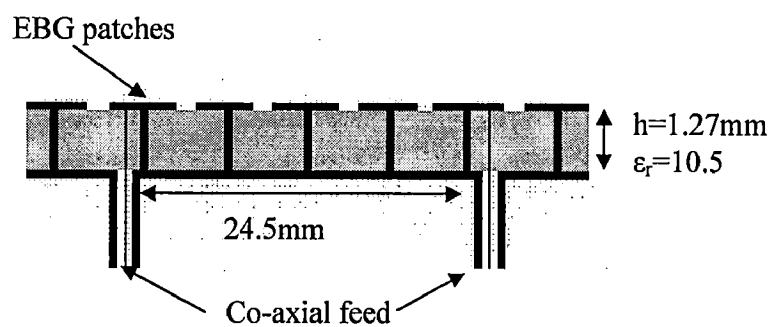


Fig. 2.20. Band gap of the EBG structure using the configuration of Fig. 2.18



*A new method for determining the Band gap* of EBG structures is shown in Fig. 2.21. This has been simulated on the IE3D simulation software to find the band gap of the proposed EBG surface. In this method, substrate of  $\epsilon_r = 10.5$  and thickness = 1.27 mm has been used. An EBG array of 3 x 5 elements with its configuration of [32323] (Fig. 2.19) has been used. Here, two coaxial feeds are used to calculate the band gap. The inner conductor of the both the coaxial line is connected to the EBG patches and the outer conductors are connected to the ground plane. In this way transmission coefficient can be obtained and is shown in Fig. 2.22. Here also, we can see that the band gap exists from 4.5 GHz to 6.4 GHz (according to the -30dB criteria).



**Fig. 2.21.** Band gap determination of EBG structure using direct feeding to EBG patches

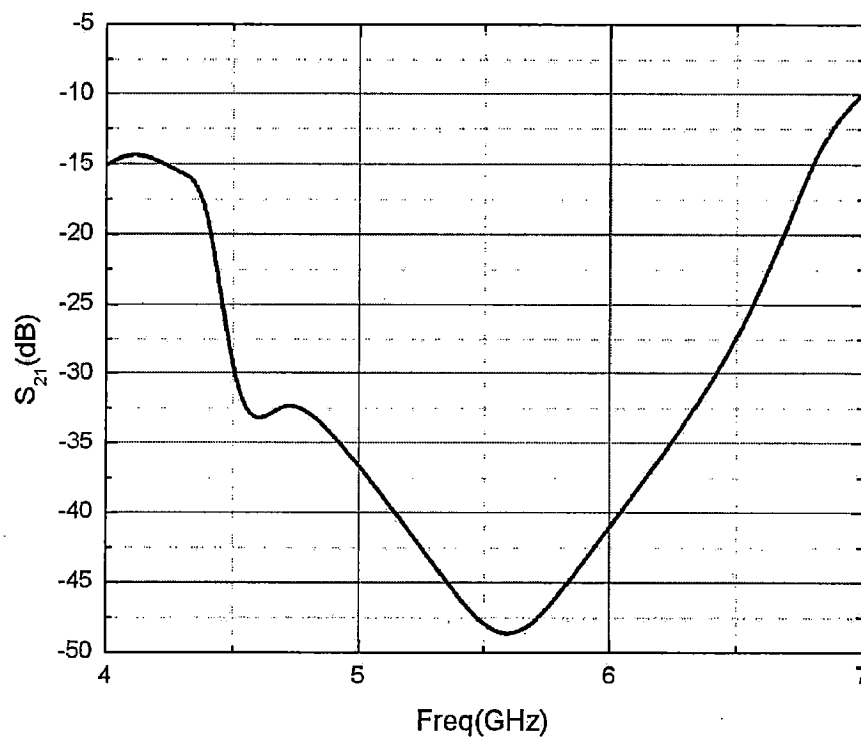


**Fig. 2.22.** Band gap calculation graph using the setup shown in Fig. 2.21

This result also matches with the previous two methods. Thus it can be concluded that for the optimized dimensions as those mentioned in section 2.5, this EBG structure operates between 4.5 GHz and 6.4 GHz. All its applications in the later chapters will be discussed in this band gap only.

### **3. MUTUAL COUPLING REDUCTION BETWEEN ARRAY ELEMENTS USING EBG**

---

---

Applications of microstrip antennas on high dielectric constant substrates are of special interest due to their compact size and conformability with the monolithic microwave integrated circuit (MMIC). However, the utilization of a high dielectric constant substrate has some drawbacks. Among these is a narrower bandwidth and pronounced surface wave excitation. The bandwidth can be increased using a thick substrate, but the excitation of surface waves increases for a thick substrate. The generation of surface waves decreases the antenna efficiency and degrades the antenna pattern. Furthermore, it increases the mutual coupling among the elements of an antenna array which causes scan blindness in a scanning array. Several methods have been proposed to reduce the effects of surface waves. One approach suggested is the synthesized substrate that lowers the effective dielectric constant of the substrate either under or around the patch [32]-[34].

This chapter mainly concentrates on the surface-wave suppression effect of the EBG structure and its application to reduce the mutual coupling of microstrip antennas in array environment.

In this chapter, the mutual coupling of probe-fed microstrip patch antenna arrays is parametrically investigated, including both the E-and H-coupling directions, on different substrate thickness and for various dielectric constants. In both coupling directions, increasing the substrate thickness will increase the mutual coupling. However, the effect of the dielectric constant on mutual coupling is different at various coupling directions. It is found that for the E-plane coupled cases the mutual coupling is stronger on a high permittivity substrate than that on a low permittivity substrate. In contrast, for the H-plane coupled cases the mutual coupling is weaker on a high permittivity substrate than that on a low permittivity substrate. This difference is due to surface waves propagating along the E-plane direction.

To reduce the strong mutual coupling of the E-plane coupled microstrip antennas on a thick and high permittivity substrate, the newly designed EBG structure is inserted between antenna elements. When the EBG parameters are properly designed, the pronounced surface waves are suppressed, resulting in a low mutual coupling. The utility

of this EBG structure is potentially useful for a variety of array applications. Fig. 3.1 shows the model to calculate the mutual coupling of probe fed microstrip antennas.

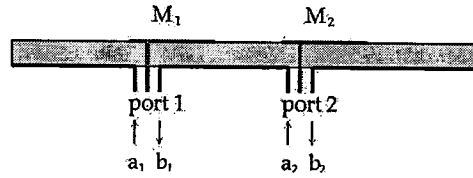


Fig. 3.1. Model to calculate the mutual coupling of probe fed microstrip antennas.

### 3.1. Mutual Coupling Comparison Of Various Microstrip Antenna Arrays

Under this section, we will analyze the mutual coupling features of microstrip antennas at different thicknesses and permittivities [35], [36]. Both the E-plane and H-plane couplings are investigated and four patch antennas are compared as follows:

1. Patch antennas on a thin and low dielectric constant substrate:  $\epsilon_r = 2.17$ ,  $h = 1$  mm and the patch size is 20.34 mm x 16.2 mm.
2. Patch antennas on a thick and low dielectric constant substrate:  $\epsilon_r = 2.17$ ,  $h = 2$  mm and the patch size is 19.7 mm x 15.8 mm.
3. Patch antennas on a thin and high dielectric constant substrate:  $\epsilon_r = 10.5$ ,  $h = 1$  mm and the patch size is 9.4mm x 7.4 mm.
4. Patch antennas on a thick and high dielectric constant substrate:  $\epsilon_r = 10.5$ ,  $h = 2$  mm and the patch size is 9 mm x 6.2 mm.

For all the cases, patch antennas were made resonant at 4.86 GHz and the separation between the patches was kept at  $0.5\lambda_{4.86 \text{ GHz}}$ , where  $\lambda_{4.86 \text{ GHz}}$  is the free space wavelength at 4.86 GHz. The frequency 4.86 GHz lies within the band gap of our proposed EBG structure (dimensions of the EBG structure have been taken to be the same as those mentioned in chapter 2). So in our next section we will show the capability of our EBG structure in suppressing the surface wave at this particular frequency.

Fig. 3.2 shows the way to measure the mutual coupling between two antenna elements in an array environment along the E-plane, as well as along the H-plane. The antennas  $M_1$  and  $M_2$ , respectively, are used as transmitting and receiving antennas and the scattering parameters  $S_{11}$  and  $S_{21}$  are measured. The entire structure has been simulated on IE3D simulation software.

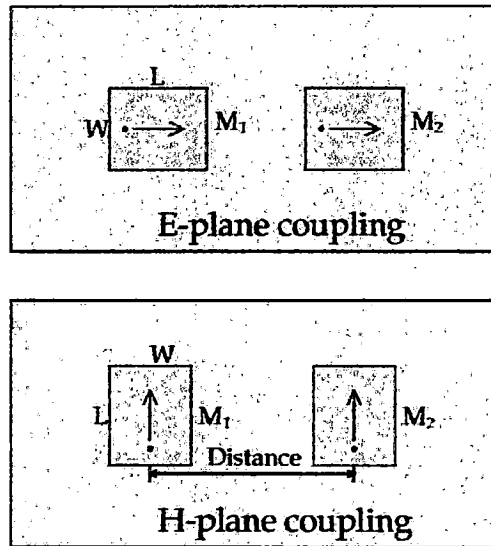


Fig. 3.2. E-and H-plane coupled probe fed microstrip antennas.

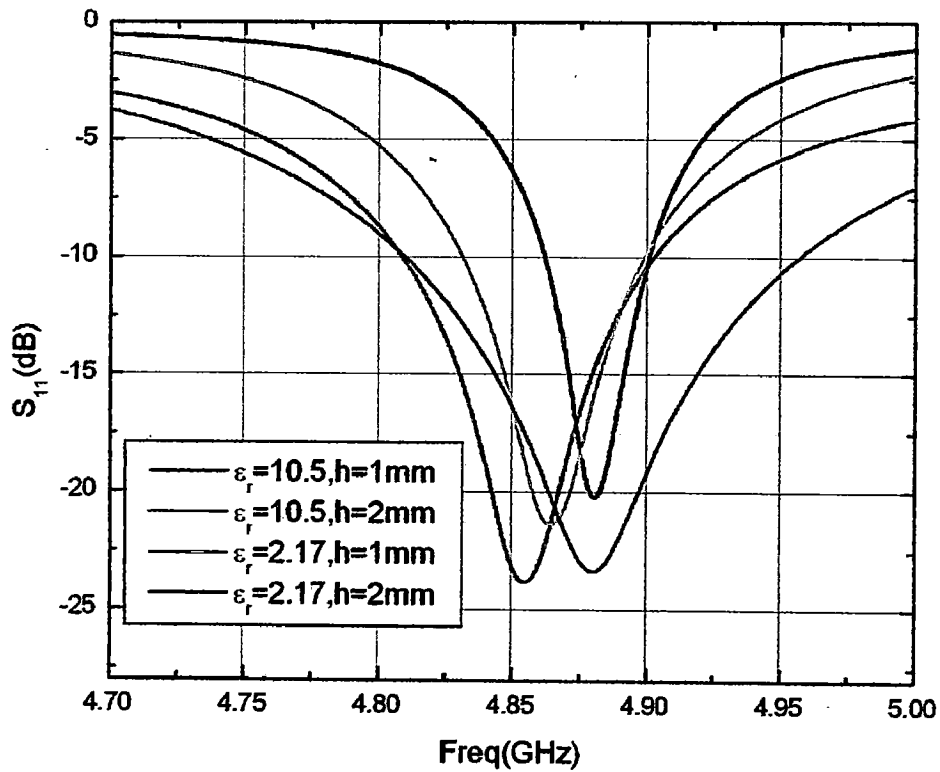


Fig. 3.3. Comparison of  $S_{11}$  versus frequency (distance  $= 0.5 \lambda_{4.86\text{GHz}}$ ) for E-plane coupled microstrip antennas on substrates of different permittivity and thickness.

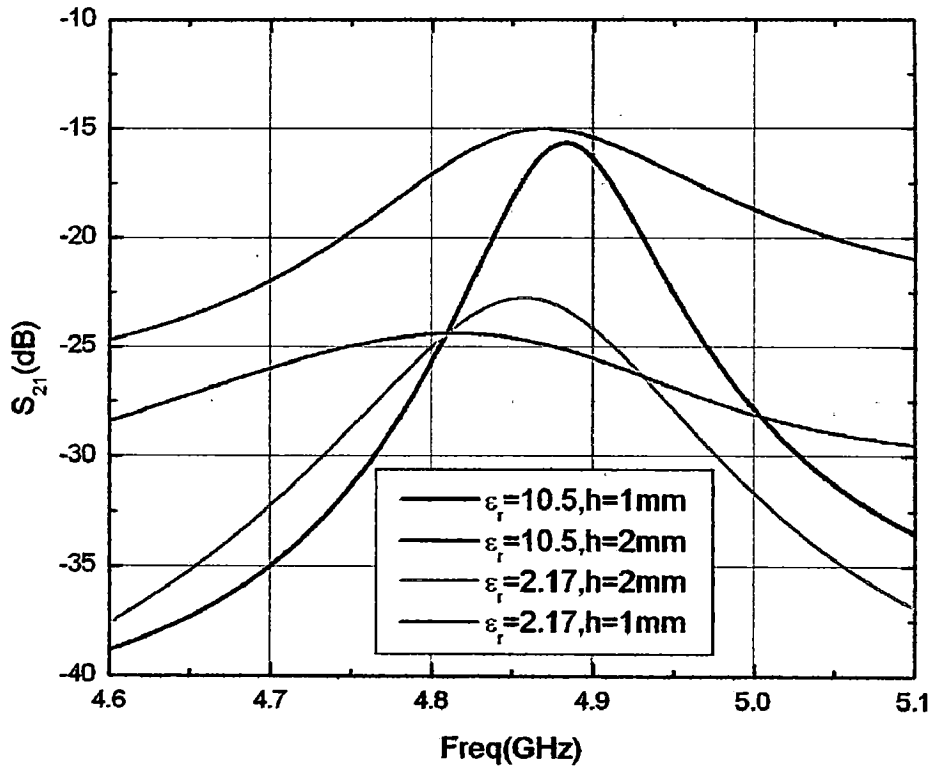


Fig. 3.4. Comparison of  $S_{21}$  versus frequency (distance  $=0.5 \lambda_{4.86 \text{ GHz}}$ ) for E-plane coupled microstrip antennas on substrates of different permittivity and thickness.

The results of the E-plane coupled microstrip antennas are depicted in Fig. 3.3. and in Fig. 3.4. Fig. 3.3 shows the return loss for the four cases considered. All the antennas were designed to resonate around 4.86 GHz. The impedance bandwidths (according to  $S_{11} < -10$  dB criterion) are 1.38% for the first case ( $\epsilon_r = 2.17, h = 1$  mm), 3.01% for the second case ( $\epsilon_r = 2.17, h = 2$  mm), 0.78% for the third case ( $\epsilon_r = 10.5, h = 1$  mm) and 1.91% for the last case ( $\epsilon_r = 10.5, h = 2$  mm). It can be observed that the bandwidth increases with increasing thickness and decreases with increasing permittivity. It can be observed that the bandwidth of case 4 is even larger than that of case 1, which means the bandwidth of microstrip antennas on a high permittivity substrate can be recovered by increasing the substrate thickness.

Fig. 3.4 presents the mutual coupling of the E-plane coupled microstrip antennas with a  $0.50 \lambda_{4.86 \text{ GHz}}$  antenna distance.  $\lambda_{4.86 \text{ GHz}}$  is the free space wavelength at the resonant frequency 4.86 GHz. The first case ( $\epsilon_r = 2.17, h = 1$  mm) has the lowest mutual coupling level, while the last case ( $\epsilon_r = 10.5, h = 2$  mm) shows the strongest. This is because the microstrip antenna on a high permittivity and thick substrate activate the most severe surface waves. It is observed that increasing the substrate thickness and permittivity will increase the mutual coupling level. This is due to the reason that surface waves propagate

along the X direction for E-plane coupled microstrip antennas and these surface waves become more severe as we increase the substrate thickness and permittivity of the substrate, resulting in a strong mutual coupling between the antenna elements.

In Fig. 3.5 and Fig. 3.6, the H-plane coupled microstrip antennas results are depicted. Fig. 3.5 shows the return loss and Fig. 3.6 shows the mutual coupling versus frequency for a  $0.50\lambda_{4.86\text{GHz}}$  antenna distance. In contrast to the E-plane coupled results, the strongest mutual coupling occurs for the second case ( $\epsilon_r = 2.17$ ,  $h = 2$  mm), which has a low dielectric constant and a thick substrate thickness. The weakest mutual coupling happens at the third case ( $\epsilon_r = 10.5$ ,  $h = 1$  mm), which has a high dielectric constant and a thin substrate thickness. It is observed that increasing the substrate thickness increases the mutual coupling, while increasing the permittivity decreases it.

This is due to the reason, that the antennas on a low permittivity substrate for the H-plane coupled microstrip antennas have a larger patch size and their fringing fields couple to each other, resulting in a strong mutual coupling. However, for the antennas on a high permittivity substrate, there is less coupling between their fringing fields due to its small patch size. The surface waves which contribute to the strong mutual coupling of the E-plane coupled case have less effect now because they do not propagate along the X direction. It can be concluded from the above discussion that the mutual coupling behavior of microstrip antennas is determined by both the directional surface waves and antenna size.

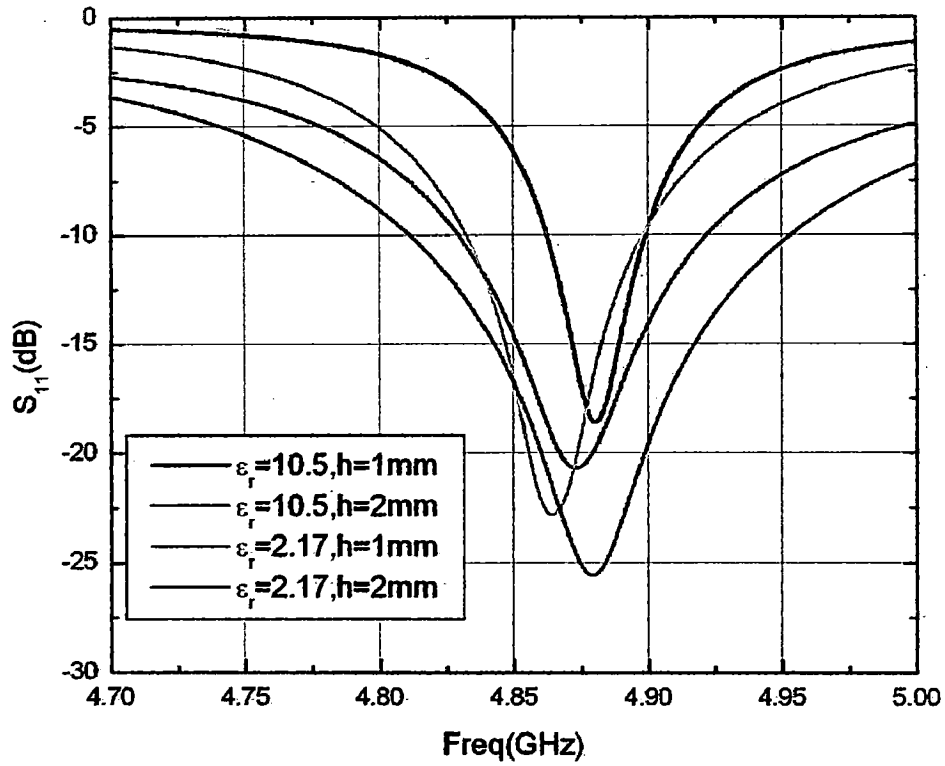


Fig. 3.5. Comparison of  $S_{11}$  versus frequency (distance  $=0.5 \lambda_{4.86 \text{ GHz}}$ ) for H-plane coupled microstrip antennas on substrates of different permittivity and thickness

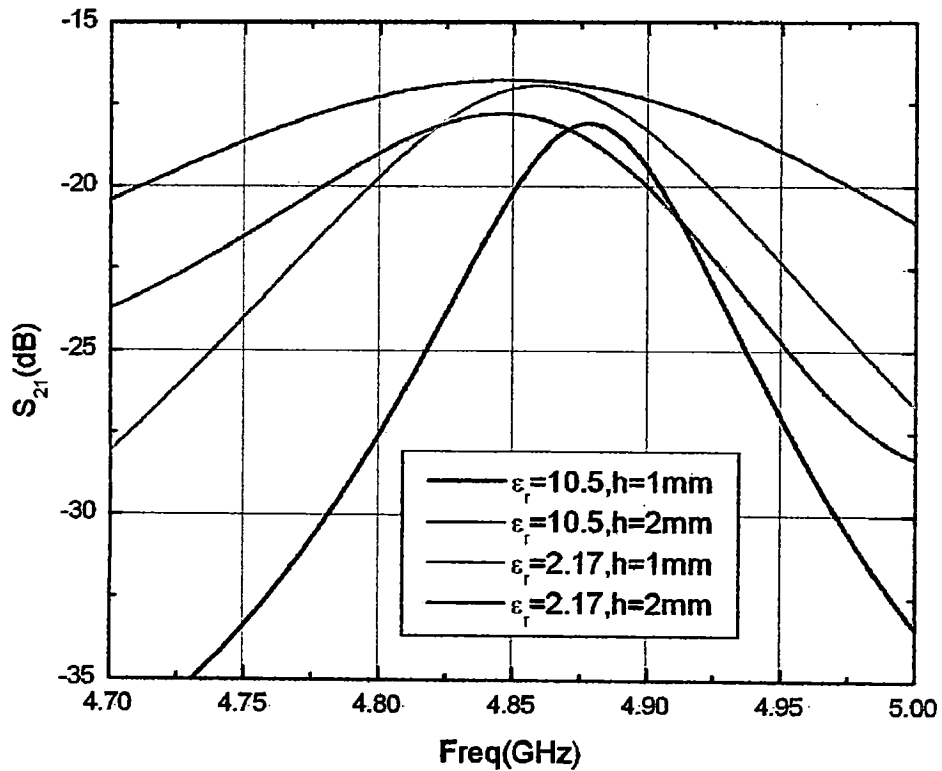
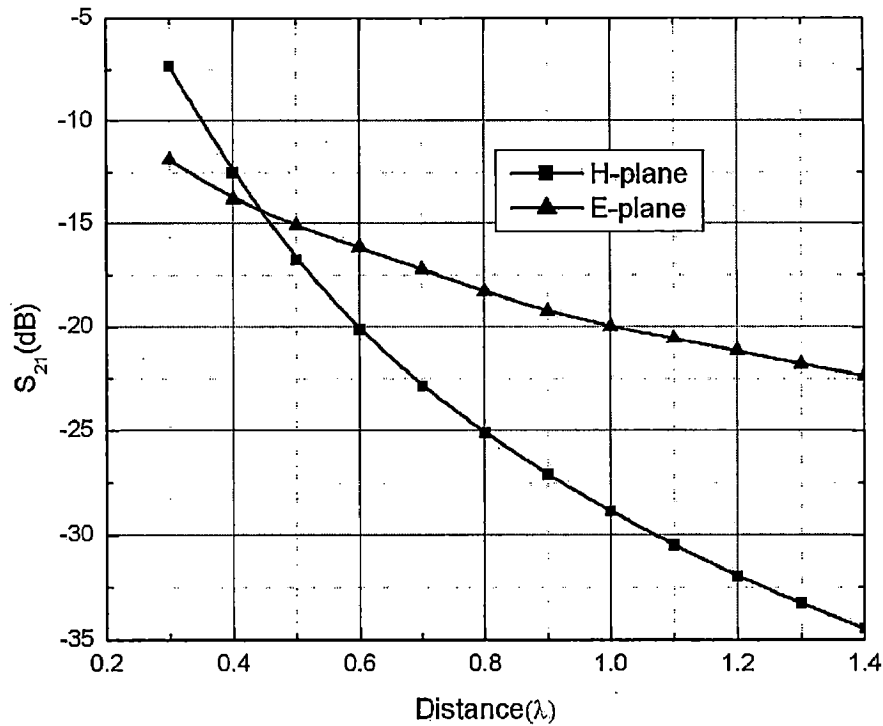


Fig. 3.6. Comparison of  $S_{21}$  versus frequency (distance  $=0.5 \lambda_{4.86 \text{ GHz}}$ ) for H-plane coupled microstrip antennas on substrates of different permittivity and thickness





**Fig. 3.7. Mutual coupling versus distance between the patches at 4.86 GHz for 9.4mm x 7 mm patches on a 1.27mm thick substrate with a dielectric constant of 10.5**

Fig. 3.7 shows the variation of mutual coupling with patch distance at the resonant frequency of 4.86 GHz for both the E-plane as well as H-plane coupled microstrip antennas for 9.4 mm x 7 mm patches on a 1.27 mm thick substrate with a dielectric constant of 10.5. The mutual coupling decreases as the antenna distance increases for both the E-plane as well as H-plane coupled microstrip antennas.

### 3.2. Mutual Coupling Reduction Using The EBG Structure

From the above comparison, it is found that the E-plane coupled microstrip antennas on a thick and high permittivity substrate exhibit very strong mutual coupling due to the pronounced surface waves. Fig. 3.8 shows the general three dimensional view of the EBG structure integrated with microstrip antenna patches in array environment. Since the EBG structure has the property to suppress surface waves in its band gap, three columns of EBG patches are inserted between the antennas to reduce the mutual coupling, as shown in Fig. 3.9. The configuration of the EBG structure that has been used is [232] (section 2.6). In the first column 2 elements are their, in the second column 3 elements are their and in the last (third) column again 2 elements are their.

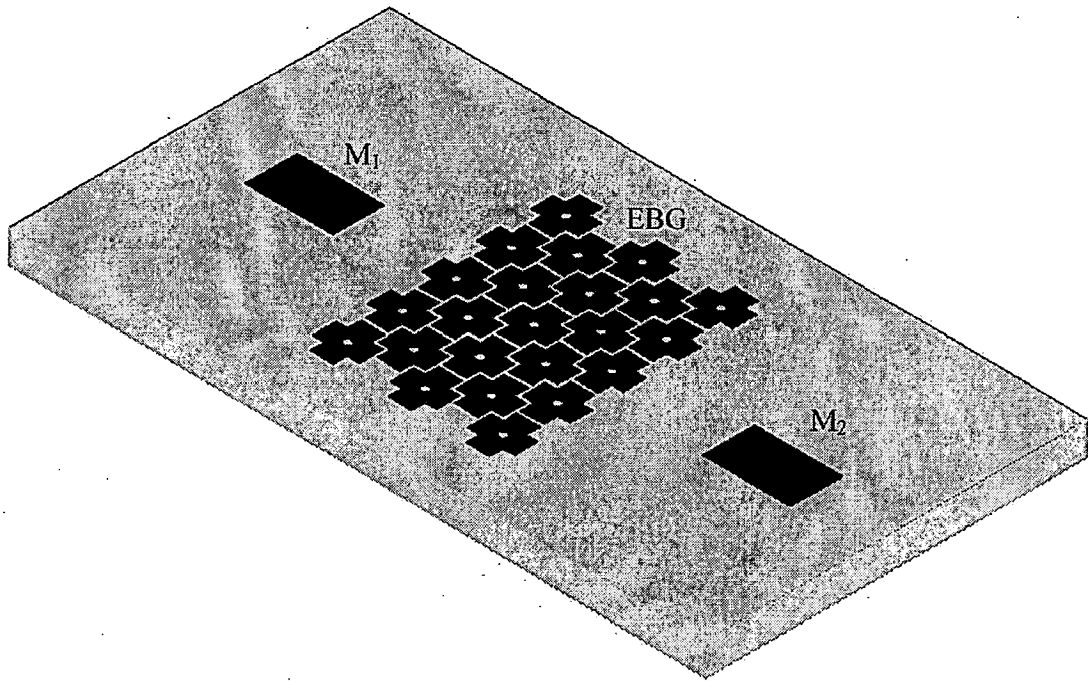


Fig. 3.8. General layout of the microstrip antennas separated by the proposed EBG structure for a low mutual coupling

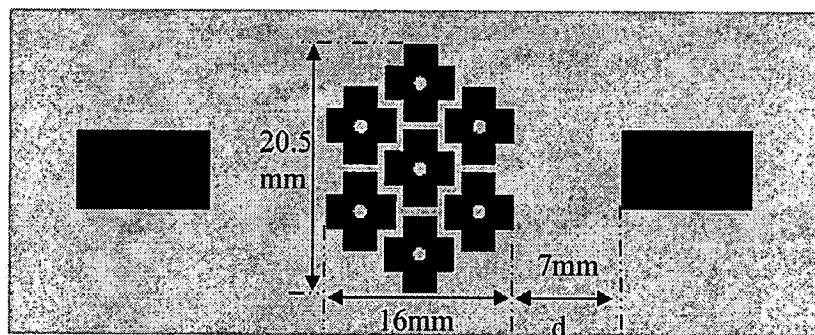


Fig. 3.9. Three column of EBG inserted between the microstrip patches

The results of mutual coupling in Fig. 3.10 are of the E-plane coupled microstrip antennas on a dielectric substrate with  $h=1.27$  mm and  $\epsilon_r=10.5$ . The patch antennas are of size 9.4 mm x 7 mm with  $0.5\lambda_{4.86 \text{ GHz}}$  distance between the patch elements of the microstrip antennas. The size of the EBG unit cell is same as designed in the second chapter 2. It can be seen from the Fig. that, without the EBG structure, the antennas show a strong mutual coupling of 16.7 dB. By employing the three layers of EBG structure, mutual coupling is greatly reduced to -23.01 dB. Thus a 6.31 dB mutual coupling reduction is observed at the resonant frequency.

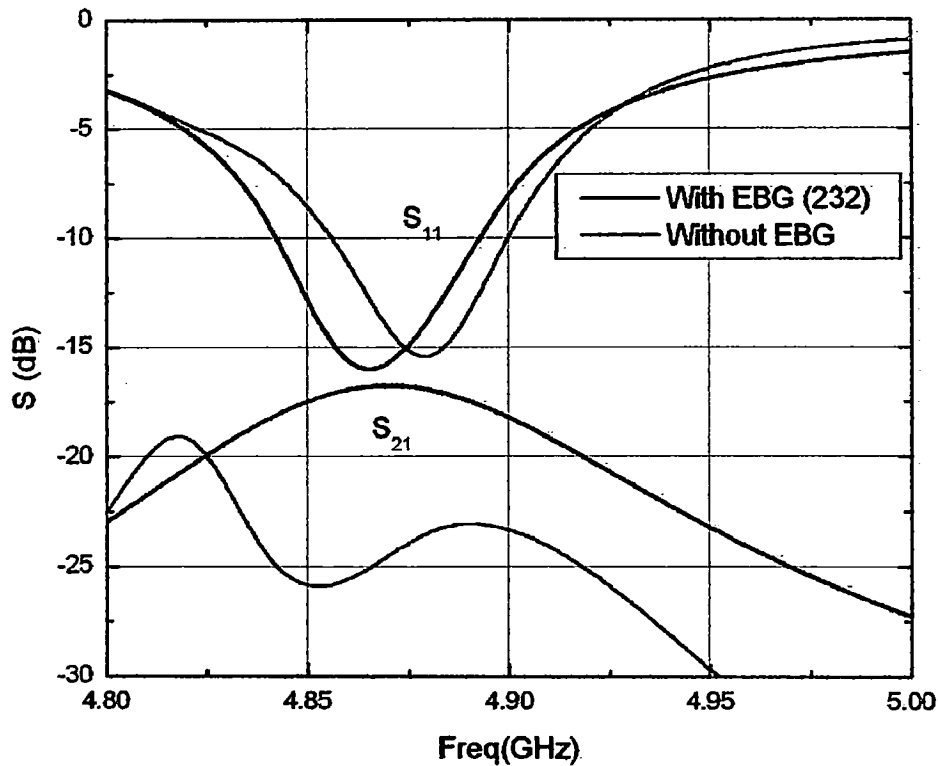


Fig. 3.10. Microstrip antenna with and without the EBG structure

### 3.3. Effect of EBG cell matrix variation on mutual coupling

Under this section we will analyze five EBG configurations and their effects on mutual coupling results in a two element array system. The antenna elements are fabricated on a dielectric substrate with  $h=1.27$  mm,  $\epsilon_r=10.5$  and the patches are of size  $9.4$  mm x  $7$  mm with  $0.5\lambda_{4.86}$  GHz distance between them. These elements are made to resonate at  $4.86$  GHz. The five EBG configurations are:

A). EBG [2323] - This represents four column of EBG elements between the microstrip antennas, where the first column has 2 elements, second column has 3 elements, third column has a 2 elements and the fourth column has 3 elements as shown in Fig. 3.11.

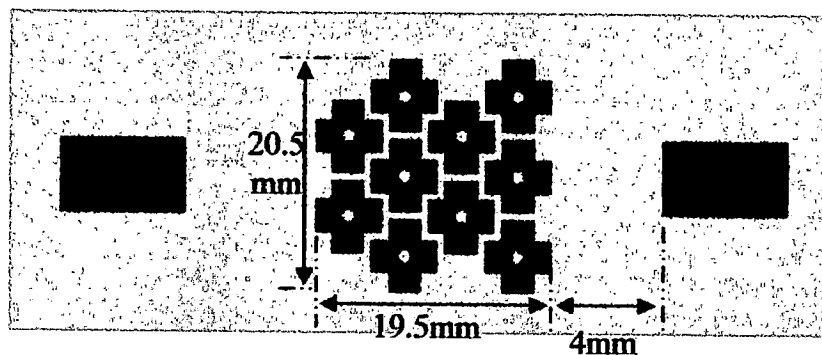
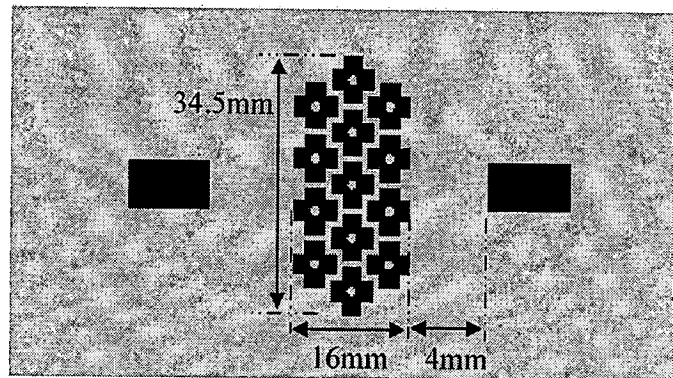


Fig. 3.11 Four columns of EBG [2323] are inserted between microstrip patches.

B). EBG [454] – This represents three column of EBG elements between the microstrip antennas, where the first column has 4 elements, second column has 5 elements and the third column has again 4 elements as shown in Fig. 3.12.



**Fig. 3.12. Three columns of EBG [454] are inserted between microstrip patches**

C). EBG [32323] – This represents five column of EBG elements between the microstrip antennas, where the first column has 3 elements, second column has 2 elements, third column has a 3 elements, fourth column has 2 elements and the fifth column has 3 elements as shown in Fig. 3.13.

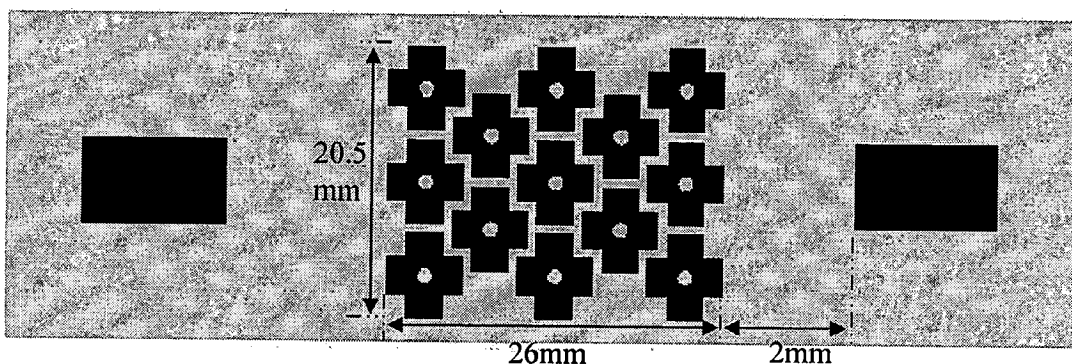


**Fig. 3.13. Five columns of EBG [32323] are inserted between microstrip patches**

D). EBG [34343] – This represents five column of EBG elements between the microstrip antennas, where the first column has 3 elements, second column has 4 elements, third column has a 3 elements, fourth column has 4 elements and the fifth column has 3 elements as shown in Fig. 3.14.

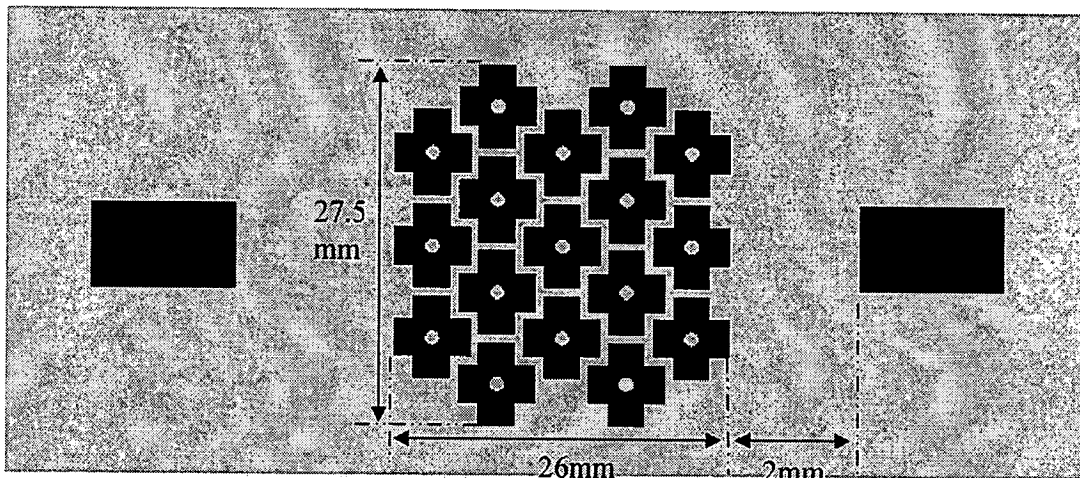


**Fig. 3.14. Five columns of EBG [34343] are inserted between microstrip patches**

E). EBG [54545] - This represents five column of EBG elements between the microstrip antennas, where the first column has 5 elements, second column has 4 elements, third column has a 5 elements, fourth column has 4 elements and the fifth column has 5 elements as shown in Fig. 3.15. The distance  $d$  between EBG and patches is 2 mm.

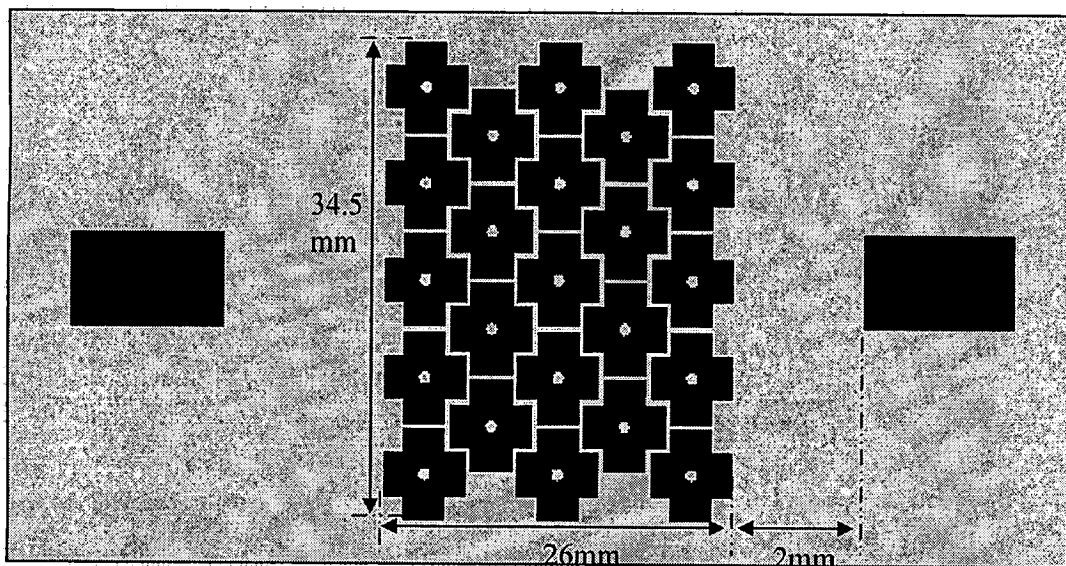


**Fig. 3.15. Five columns of EBG [54545] are inserted between microstrip patches.**

Fig. 3.16 shows the mutual coupling results for the two element array without the EBG structure and with the different configuration of EBG structures. It is observed that all the antennas resonate around 4.86 GHz. Although the existence of the EBG has some effects on the input matches of the antennas, all the antennas still have better than -10 dB matches.

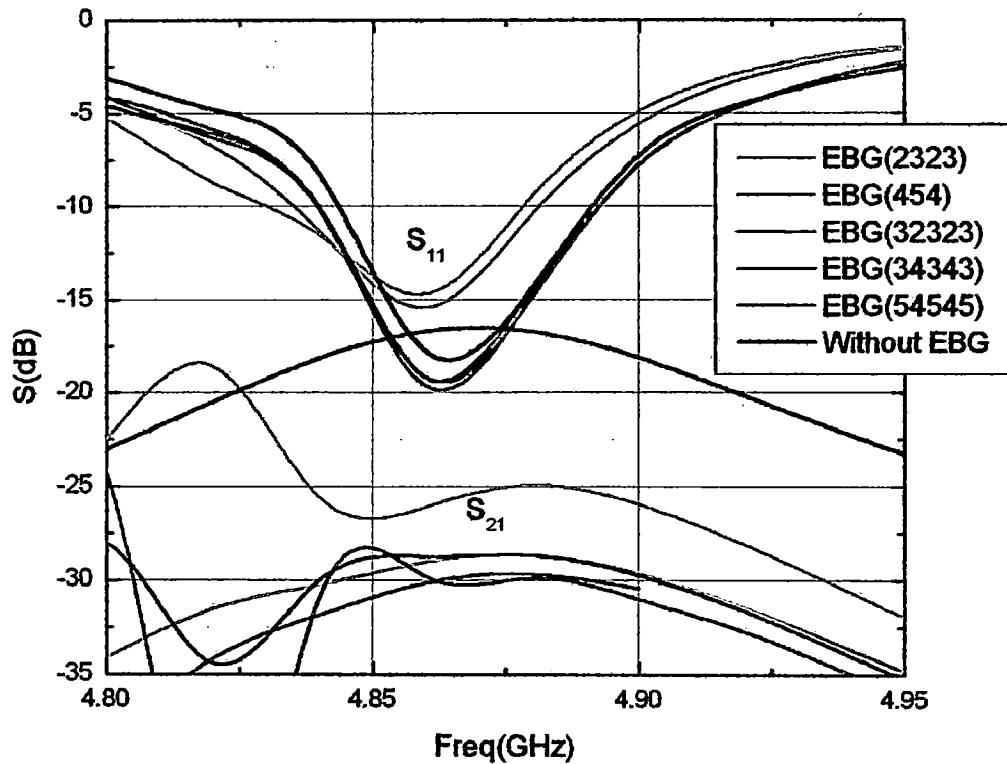


**Fig. 3.16. Variation in Mutual coupling( $S_{21}$ ) with different layer of EBG(abcd) where number of literals represent the number of columns and the values of the literals (a,b,c,d) represents the number of elements of the unit cell in that columns .**

Without the EBG structure, the antennas show a strong mutual coupling of 16.7 dB as shown in Fig. 3.16. If the EBG structures are employed, the mutual coupling level changes. The resonant frequency 4.86 GHz falls inside the EBG band gap so that the surface waves are suppressed. As a result, the mutual coupling is greatly reduced. It can be seen from Table 3.1 that as the number of EBG column increases, reduction in mutual coupling increases, also by increasing the total number of elements in the EBG array, further reduction in mutual coupling is seen to occur. Values of mutual coupling for various EBG configuration is shown in Table 3.1.

**Table 3.1. Effect of EBG cell matrix configuration on mutual coupling**

| EBG configuration | Mutual coupling $S_{21}$ | Improvement in $S_{21}$ over the case without the EBG structure |
|-------------------|--------------------------|---|
| EBG(2323)         | -28.83                   | 12.13 dB  |
| EBG(454)          | -26.07                   | 9.37 dB   |
| EBG(32323)        | -29.08                   | 12.38 dB  |
| EBG(34343)        | -28.74                   | 12.04 dB  |
| EBG(54545)        | -30.13                   | 13.43 dB  |

Finally, it can be concluded that the proposed EBG structure can be utilized to reduce the mutual coupling between array elements in the stop band from 4.5 GHz to 6.4 GHz.

## **4. EFFECT OF THE PROPOSED EBG SURFACE ON THE RADIATION CHARACTERISTICS OF A DIPOLE ANTENNA**

---

---

It is known that the reflection phase of an EBG surface varies continuously from  $180^\circ$  to  $-180^\circ$  versus frequency, not only  $180^\circ$  for a PEC surface or  $0^\circ$  for a PMC surface. This reflection phase feature makes EBG surfaces unique. One potentially important application of this surface is its usage in replacing the conventional perfect electric conductor (PEC) ground plane with an EBG ground plane for a low profile wire antenna design, which is desirable in many wireless communication systems. For this design, the operational frequency band of an EBG structure is defined as the frequency region within which a low profile wire antenna radiates efficiently, namely, having a good return loss and radiation patterns [23].

This operational frequency region is the region where the EBG surface has a reflection phase in the range  $90^\circ \pm 45^\circ$  and in this frequency band EBG surface don't behave like the PMC or PEC surface [23]. This quadratic reflection phase allows a low profile wire antenna to obtain a good return loss.

### **4.1. Comparison of the PEC, Free Space and EBG Ground Planes**

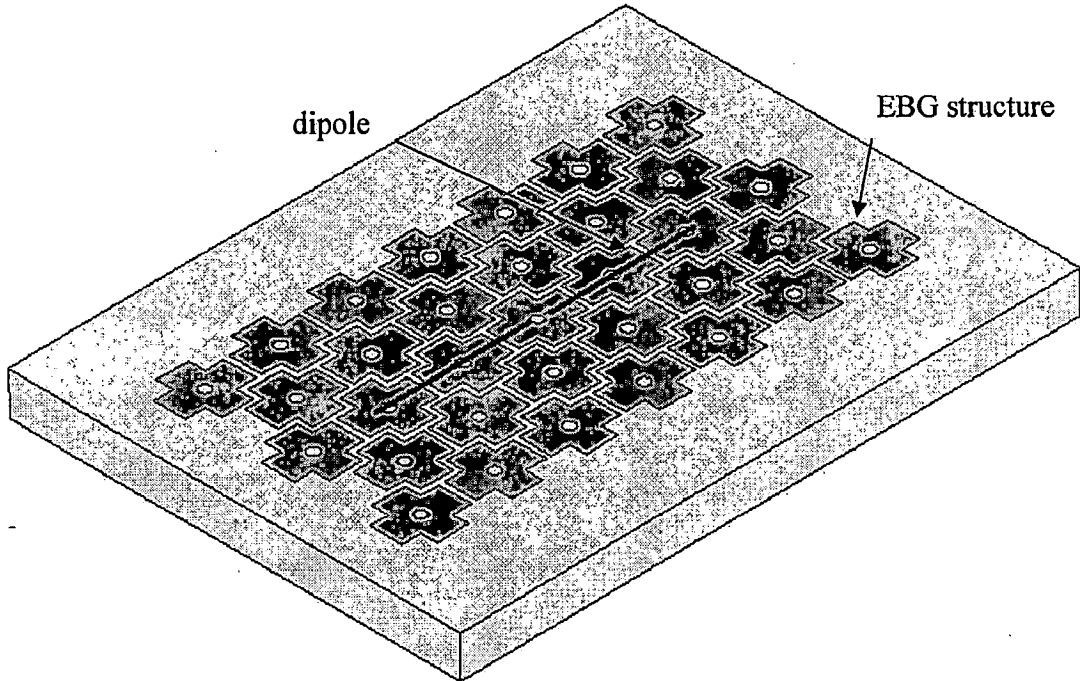
In wireless communications, it is desirable for antennas to be of low profile. The low profile design usually refers to the antenna structures whose overall height is less than one tenth of the wavelength at the operating frequency. In this section the PEC, Free Space and EBG surfaces are each used as the ground plane to compare their capabilities for low profile antenna designs.

Fig. 4.1 shows a dipole antenna over the EBG ground plane and Fig. 4.2 shows a dipole antenna over a PEC ground plane. The side view for the EBG case is shown in Fig. 4.3 and the side view for the PEC case is shown in Fig. 4.4. The top view of the Dipole over EBG structure is shown in Fig. 4.5.

For the case when the dipole is above the EBG surface, we keep the parameters of the EBG surface fixed (dimensions of the EBG structure has been taken to be the same as those mentioned in chapter 2) and then we continuously change the length of the dipole. Now for different lengths, dipole will resonate at different frequencies. Because the



reflection phase of the EBG surface changes with frequency, the return loss of the dipole will also change. Thus, for a suitable reflection phase of the EBG surface, this dipole can achieve a good return loss. In addition to observing the return loss, we also observe the radiation pattern of the dipole to evaluate the radiation efficiency.



**Fig. 4.1.** Low profile dipole antenna over a finite EBG ground plane.

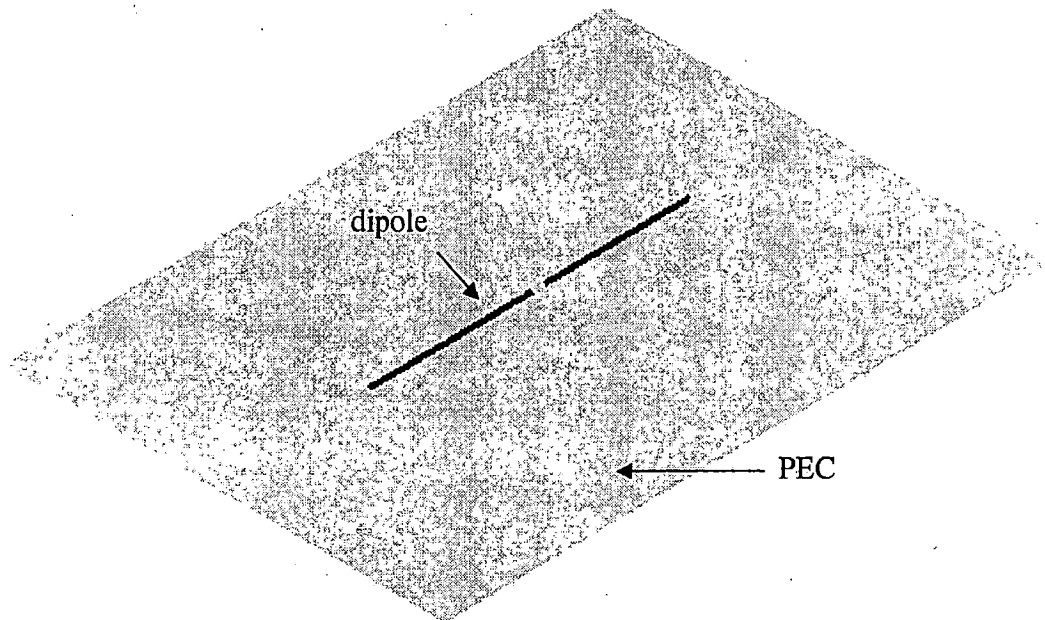


**Fig. 4.2.** Dipole antenna over the PEC ground plane

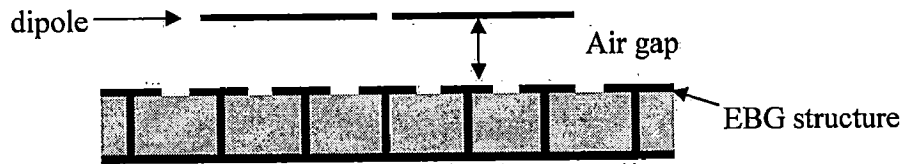


Fig. 4.3. Side view of the dipole antenna over the EBG ground plane

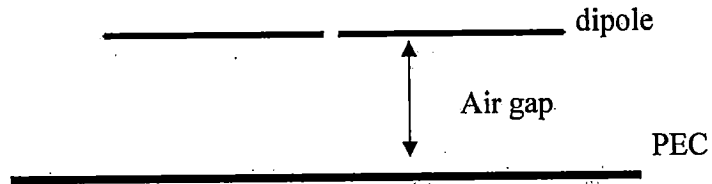


Fig. 4.4. Side view of the dipole antenna over the PEC ground plane

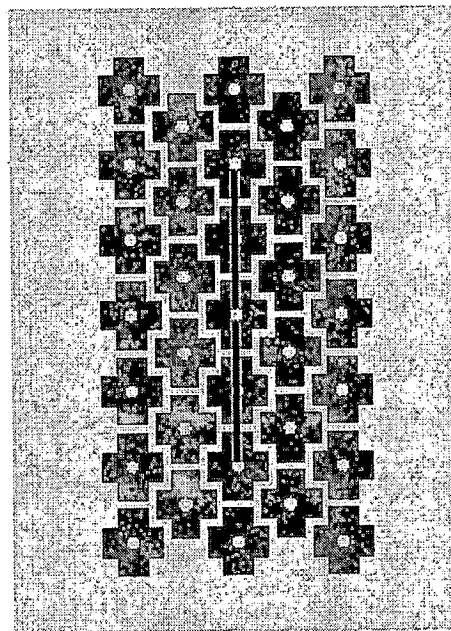


Fig. 4.5. Top view of the dipole antenna over the EBG ground plane

By continuously observing the return loss and the radiation pattern of the dipole for various lengths, we found that at a frequency of 5.27 GHz we obtain a good return loss of -29.85dB and at the same time the antenna exhibited an increased front-to-back ratio. For this particular frequency, the length of the dipole is  $0.453\lambda_{5.27}$  and its radius  $0.003\lambda_{5.27 \text{ GHz}}$ , where  $\lambda_{5.27 \text{ GHz}}$  is the free space wavelength at 5.27 GHz. A finite ground plane with  $1 \lambda_{5.27 \text{ GHz}} \times 1 \lambda_{5.27 \text{ GHz}}$  size is used in this analysis and the overall height of the dipole from the bottom ground plane of the EBG structure is found to be  $0.105\lambda_{5.27 \text{ GHz}}$ . Here, the height of the dipole over the top surface of the EBG ground plane is  $0.083\lambda_{5.27 \text{ GHz}}$  and the

height of the EBG ground plane is  $0.022\lambda_{5.27 \text{ GHz}}$ . This makes the overall height to be  $0.105\lambda_{5.27 \text{ GHz}}$ . An EBG configuration of 76767 has been used as shown in Fig. 4.5. This frequency of 5.27 GHz lies within the band gap and is close to the resonant frequency of the EBG structure. So we get optimum performance for this particular frequency only.

In order to compare the performance of the dipole over the EBG ground plane and over the PEC ground plane, we again place the dipole over a PEC ground plane keeping all the parameters same (same height between dipole and PEC and same dipole length). Fig. 4.6 compares the return loss of a dipole antenna over a PEC, Free Space and EBG ground plane. The input impedance is matched to a  $50\Omega$  transmission line. With the PEC surface as the ground plane, the return loss of the dipole is only  $-9.32\text{dB}$ . This is because the PEC surface has an  $180^\circ$  reflection phase, so that the direction of the image current is opposite to that of the original dipole. The reverse image current impedes the efficiency of the radiation of the dipole, resulting in a very poor return loss. For the case when the dipole is placed in Free Space, it has a return loss of  $-15.46\text{dB}$ .

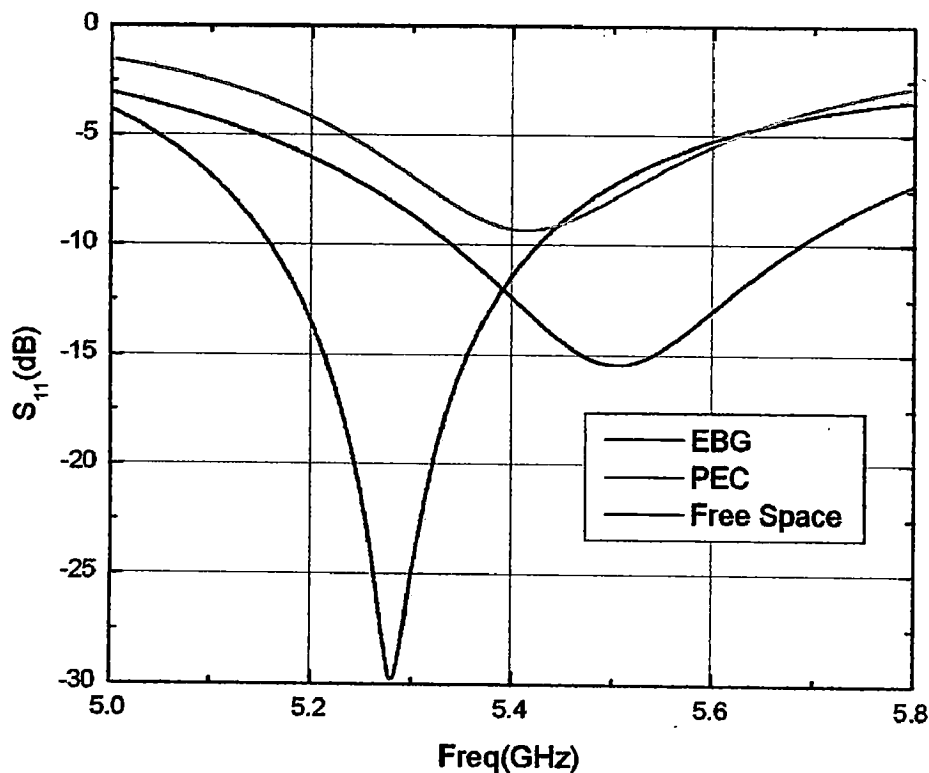


Fig. 4.6. Return Loss of the dipole antenna over the PEC, Free space and EBG ground planes.

The best return loss of -29.85dB is achieved by the dipole antenna over the EBG ground plane. From this comparison, it can be seen that the EBG surface is a good ground plane candidate for a low profile wire antenna design. It has been observed that there is a shift in frequency, which is mainly because of the difference in the relative permittivity of the medium as EBG structure is on a substrate of permittivity of 10.5. Because of this, the resonant frequency shifts downwards.

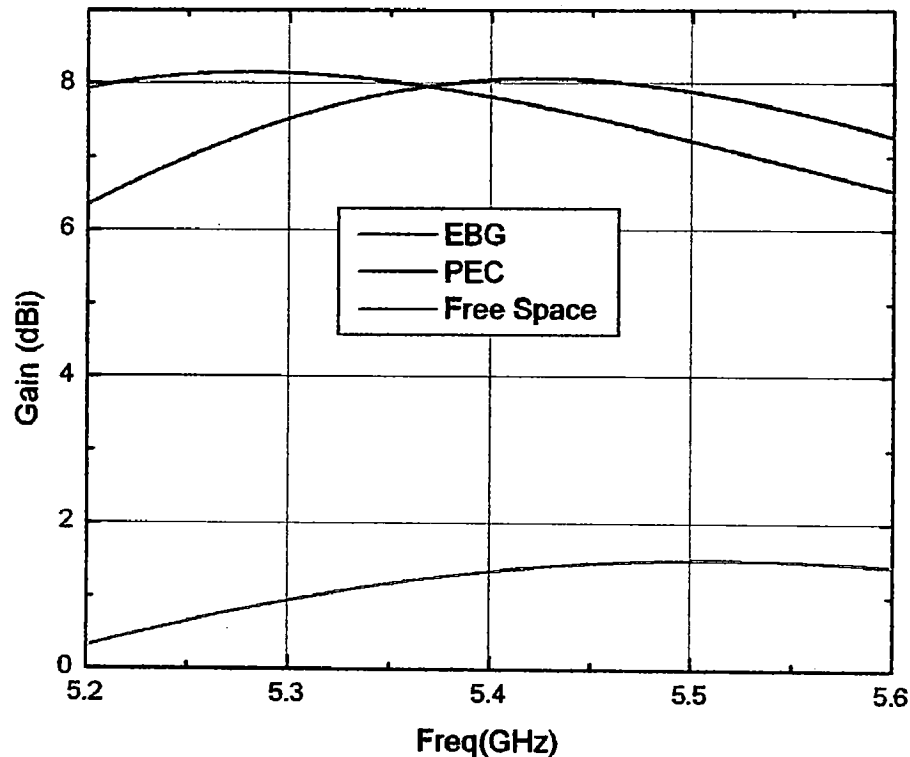
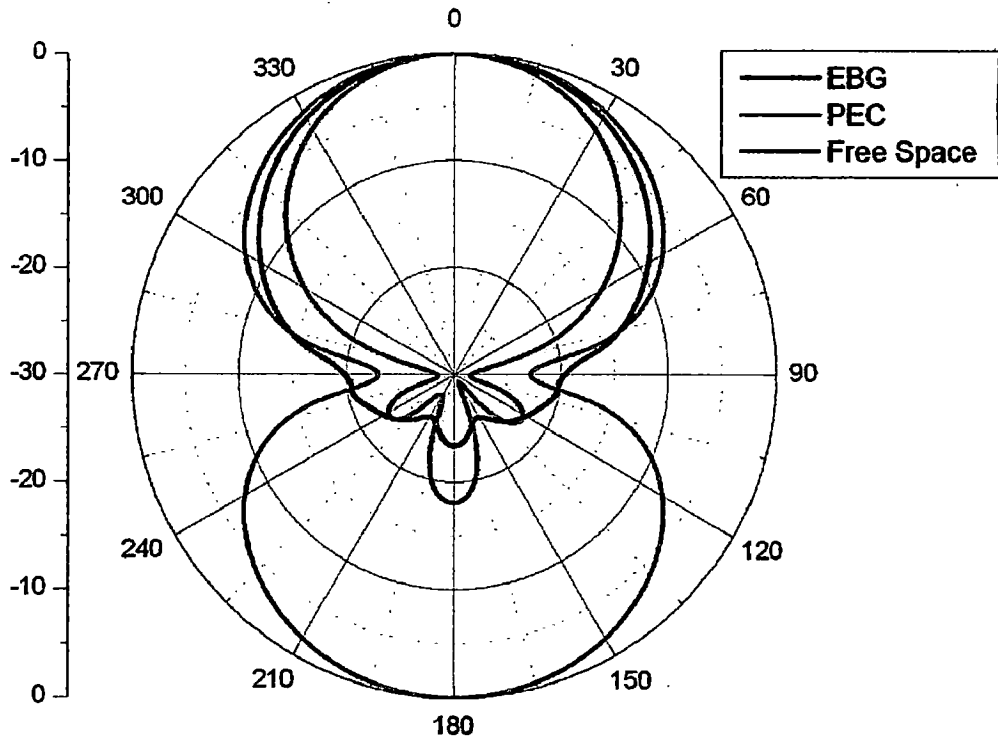
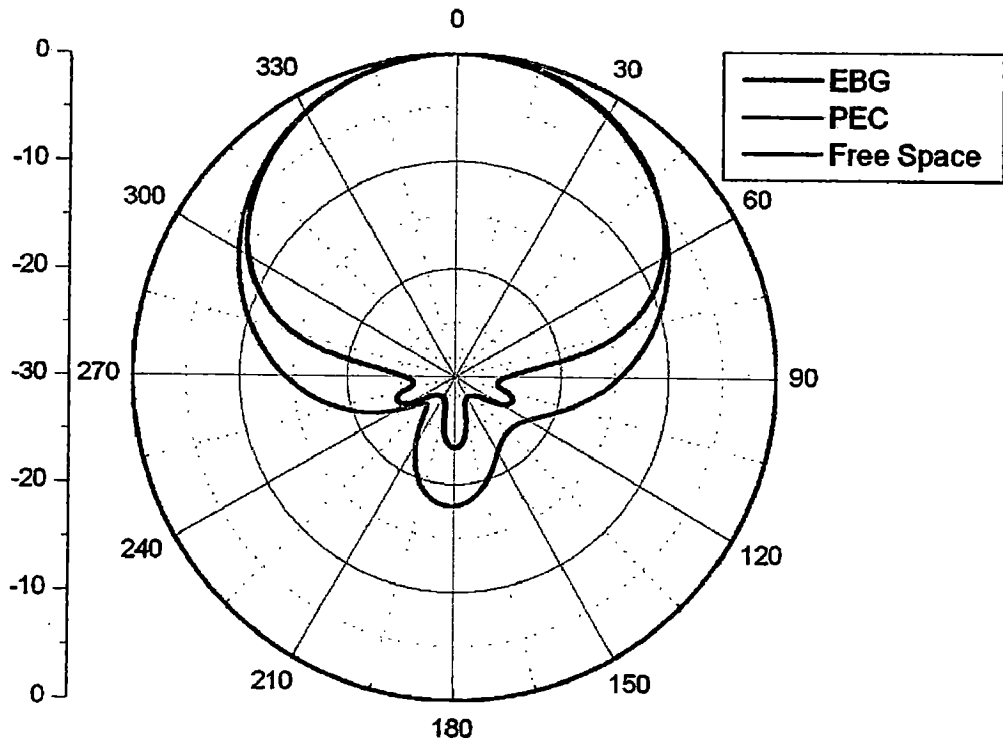


Fig. 4.7. Gain of the dipole antenna over the PEC, Free space and EBG ground planes.

Gain comparison has also been carried out for all the three cases for the same dimensions. For the case when the dipole is above the EBG surface, a maximum gain of 8.15 dBi is obtained at its resonant frequency of 5.27 GHz, while for the case when the dipole is above the PEC plane, a maximum gain of 8.41 dBi is obtained at its resonant frequency of 5.42 GHz. When the dipole is in free space, a maximum gain of 1.5 dBi is obtained at its resonant frequency of 5.5 GHz. Thus it can be seen that in terms of gain, both the EBG case as well as PEC case offer the same advantage.



**Fig. 4.8. E-plane radiation pattern**



**Fig. 4.9. H-plane radiation pattern**

Fig. 4.8 displays the E-plane and Fig. 4.9 displays H-plane patterns for the cases when the dipole is placed above the EBG surface, above the PEC surface and in Free Space. As can be seen from the figures, the back radiation has been considerably reduced when the

dipole antenna is above the EBG ground plane or when it is above the perfect electric conductor. But the front-to-back ratio is better for the case of EBG as compared to PEC case. For EBG case, the front-to-back ratio is 23.29 dB, while for the PEC case, the front-to-back ratio is 17.96 dB. Thus, an improvement of 5 dB in front-to-back ratio is obtained when we use EBG as compared to PEC. Also, the 3 dB beamwidth for the EBG case is  $70^\circ$  while for the PEC case it is  $60^\circ$ . So it can be clearly seen that the EBG has the advantage over the PEC in terms of 3 dB beamwidth as well as in terms of front-to-back ratio and at the same time antenna height is greatly reduced for the EBG case as compared to that in the PEC case.

## 5. EFFECT OF EBG SURFACE ON THE RADIATION CHARACTERISTICS OF A MICROSTRIP SLOT ANTENNA

---

---

Printed slot antennas have been extensively studied and offer a number of advantages due to their low profile, low-cost, lightweight, ease of fabrication and ease of integration with electronics. Their main drawback, however, is that they are inherently bi-directional radiators, with the back radiation being undesirable.

One technique commonly employed to reduce the back-radiation is the addition of a metallic reflector in order to redirect the back radiation forward. The main drawback in this case is that the geometry of the antenna is now transformed into a parallel-plate environment resulting in the excitation of the parallel-plate (dominant) transverse electromagnetic (TEM) mode which drastically degrades the radiation efficiency as well as the antenna patterns. In addition, the reflector must be placed a quarter-wavelength away from the slot ground-plane for proper operation so that the reflected back radiation incurs an additional phase of  $360^\circ$  and thus adds in phase with the forward directed radiation.. However, because of the quarter wavelength distance, the resulting structure is not low-profile at lower RF frequencies.

The back radiation can be reduced by backing the slot with an electromagnetic band gap surface, instead of the uniform conducting reflector.

Since the EBG structures exhibit stop bands, where electromagnetic wave propagation is evanescent, any electromagnetic disturbance that is excited in such a structure will not propagate if its frequency constituents lie within the stop band of the EBG structure. Using the above concept it can be expected that if a slot antenna is designed to resonate in the stop band of a properly designed EBG structure (i.e., with a band-gap), the parallel-plate mode will become evanescent. Hence, in such an arrangement, the front-to-back lobe ratio and the patterns should improve compared to the case of a simple conductor-backed slot. A few recent research works have utilized such an approach [31].

In this chapter a rectangular-slot antenna with a resonance near the center of the EBG surface stop band was chosen as the radiating element. The printed rectangular-slot was placed 4 mm away from the EBG surface (distance from EBG ground) and this combined

structure constituted the new uni-directional antenna. An additional advantage compared to the standard conductor plane backing, is that the EBG surface can be placed close to the slot antenna ( $\ll \lambda/4$ ) and hence, a low profile can be achieved.

### 5.1. Rectangular-slot antenna

The three dimensional view of the rectangular-slot antenna is shown in Fig. 5.1. The top view of the same antenna is shown in Fig. 5.2 and the side view is shown in Fig. 5.3.

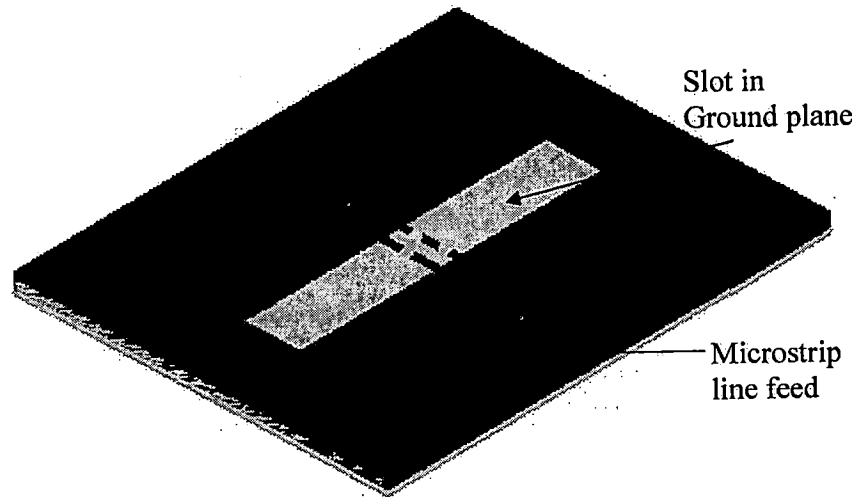


Fig. 5.1. Three dimensional view of the rectangular-slot antenna

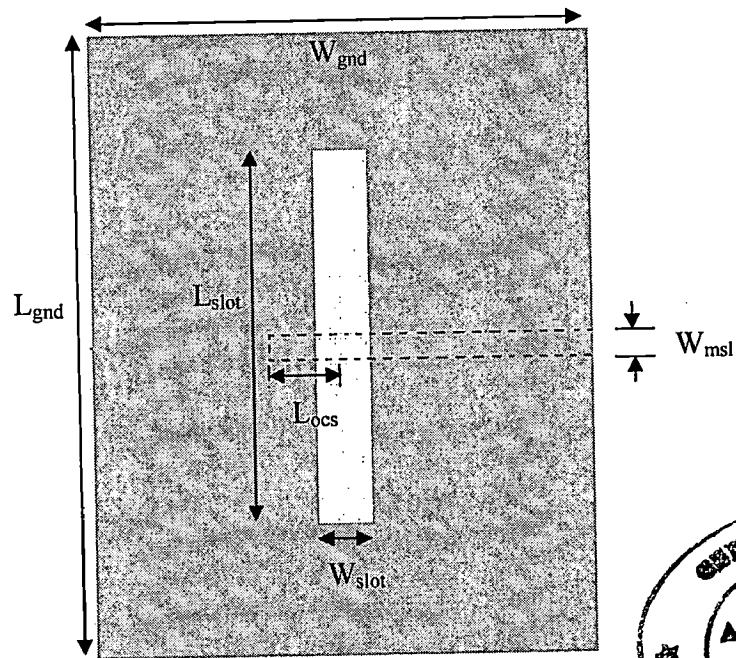
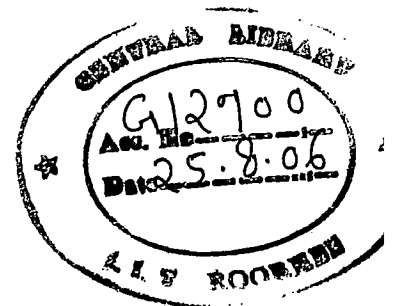
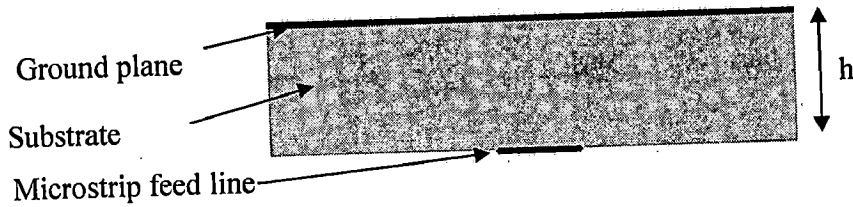


Fig. 5.2. Top view of the rectangular-slot antenna







**Fig. 5.3. Side view of the rectangular-slot antenna**

Here, in order to achieve proper impedance match, tuning of slot width, slot length and length of the open circuit stub has been carried out and the final optimized parameters for the rectangular-slot antenna are:

|   |          |
|---|----------|
| Feed line width ( $W_{msl}$ )                 | 1.146 mm |
| Length of the open circuit stub ( $L_{ocs}$ ) | 7.55 mm  |
| Slot width ( $W_{slot}$ )                     | 4.7 mm   |
| Slot length ( $L_{slot}$ )                    | 25.4 mm  |
| Ground plane width ( $W_{gnd}$ )              | 16 mm    |
| Ground plane length ( $L_{gnd}$ )             | 36 mm    |
| Substrate thickness ( $h$ )                   | 1.27 mm  |
| Substrate permittivity ( $\epsilon_r$ )       | 10.5     |

For the above parameters, rectangular slot antenna resonates at 5.32 GHz as shown in Fig. 5.4, which lies within the band gap of the EBG surface. The bandwidth referred to the -10 dB return loss is found to be 8.43%.

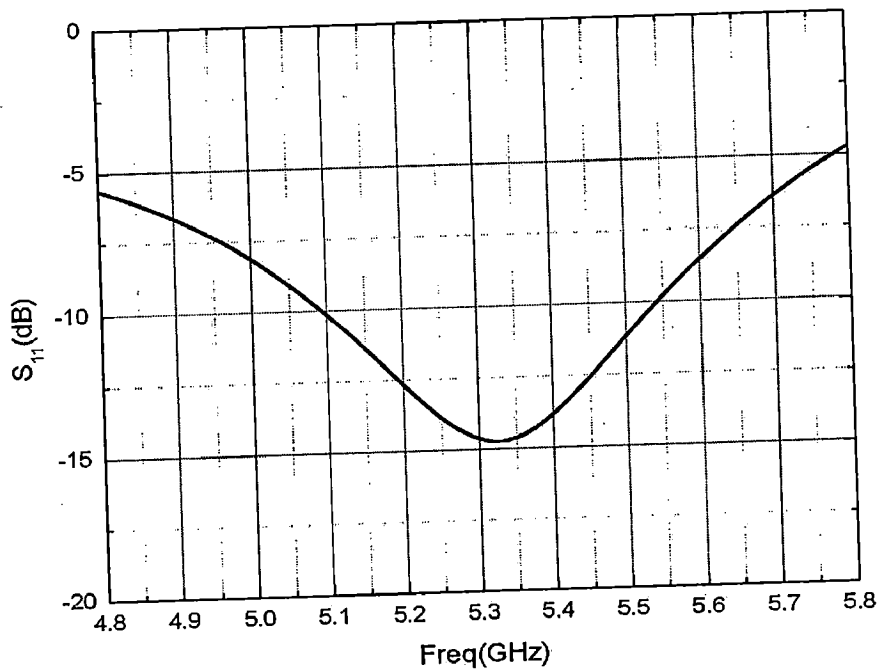


**Fig. 5.4. Return loss of the slot antenna with EBG Reflector**

## 5.2. EBG backed Rectangular-slot antenna

The three dimensional view of the EBG backed rectangular slot antenna is shown in Fig. 5.5. Its front view is depicted in Fig. 5.6 and the top view of the lower substrate carrying EBG structure over it is shown in Fig. 5.7. The rectangular slot antenna is backed by the EBG surface with 2.73 mm air gap between the EBG and the antenna substrate.

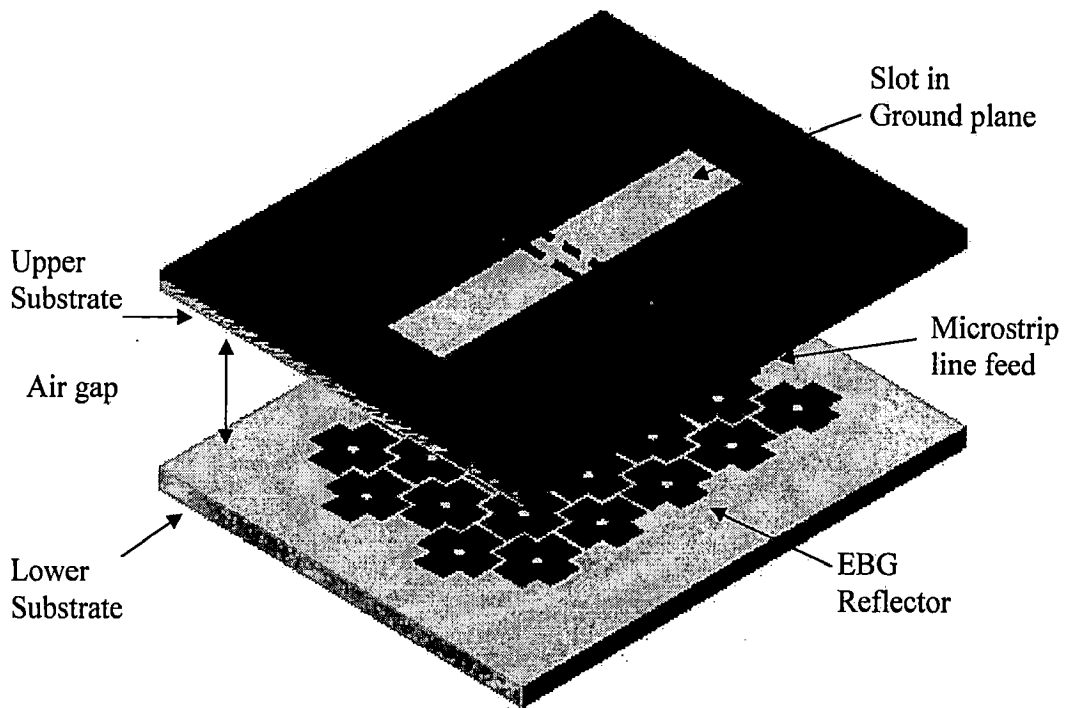


Fig. 5.5. Three dimensional view of the EBG backed rectangular-slot antenna

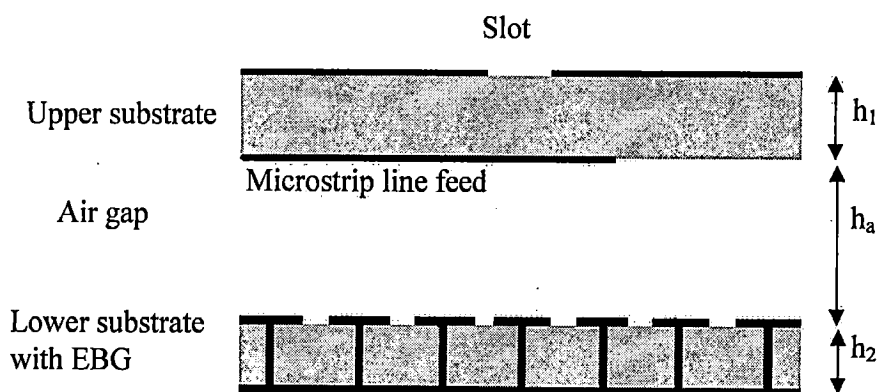
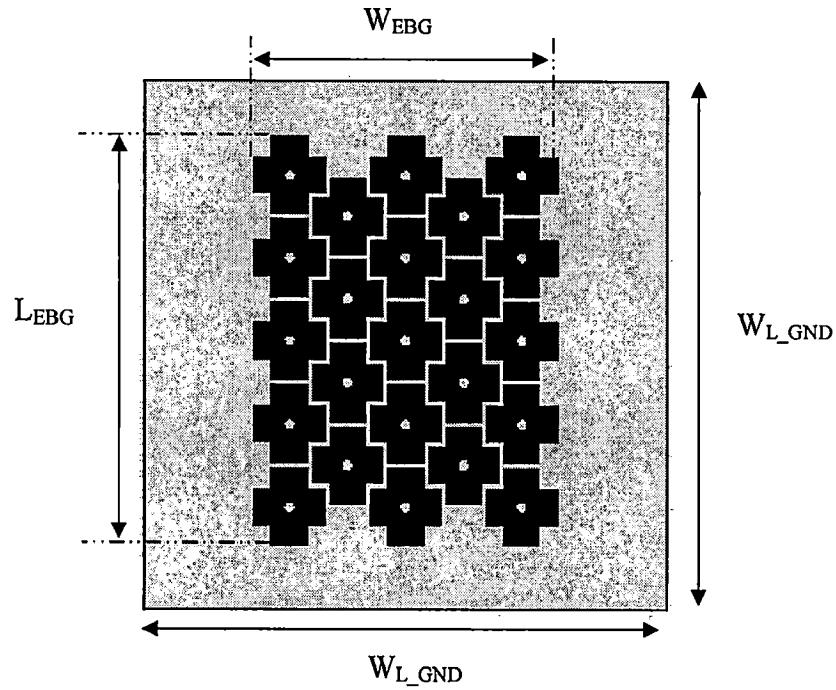


Fig. 5.6. Front view of the EBG backed rectangular-slot antenna



**Fig. 5.7. Top view of the lower substrate having EBG over it**

With the introduction of the EBG, an impedance mismatch is observed in the original slot antenna configuration. In order to establish the impedance matching, tuning of the slot antenna parameters is carried out. The tuned rectangular-slot antenna with its relevant dimensions is shown below.

|   |          |
|---|----------|
| Feed line width ( $W_{msl}$ )                           | 1.146 mm |
| Length of the open circuit stub ( $L_{ocs}$ )           | 6.9 mm   |
| Slot width ( $W_{slot}$ )                               | 3 mm     |
| Slot length ( $L_{slot}$ )                              | 28.4 mm  |
| Upper Ground plane width carrying slot ( $W_{gnd}$ )    | 16 mm    |
| Upper Ground plane length carrying slot ( $L_{gnd}$ )   | 36 mm    |
| Lower Ground plane width carrying EBG ( $W_{l\_gnd}$ )  | 28 mm    |
| Lower Ground plane length carrying EBG ( $L_{l\_gnd}$ ) | 36 mm    |
| EBG width ( $W_{EBG}$ )                                 | 26 mm    |
| EBG length ( $L_{EBG}$ )                                | 34.5 mm  |
| Air gap ( $h_a$ )                                       | 2.73 mm  |

The antenna was simulated on the finite ground plane of size 28 x 36 mm and the EBG surface of array size 5 x 4 with its configuration of 54545 is used as shown in Fig. 5.7. The dimensions of the EBG structure used here are same as those mentioned in chapter 2. The placement of the EBG surface relative to the antenna substrate is also shown in Fig. 5.5. The return loss of the EBG backed antenna exhibited a resonance at 5.44 GHz as shown in Fig. 5.8. The bandwidth referred to the -10 dB return loss for the above antenna is found to be 10.62%.

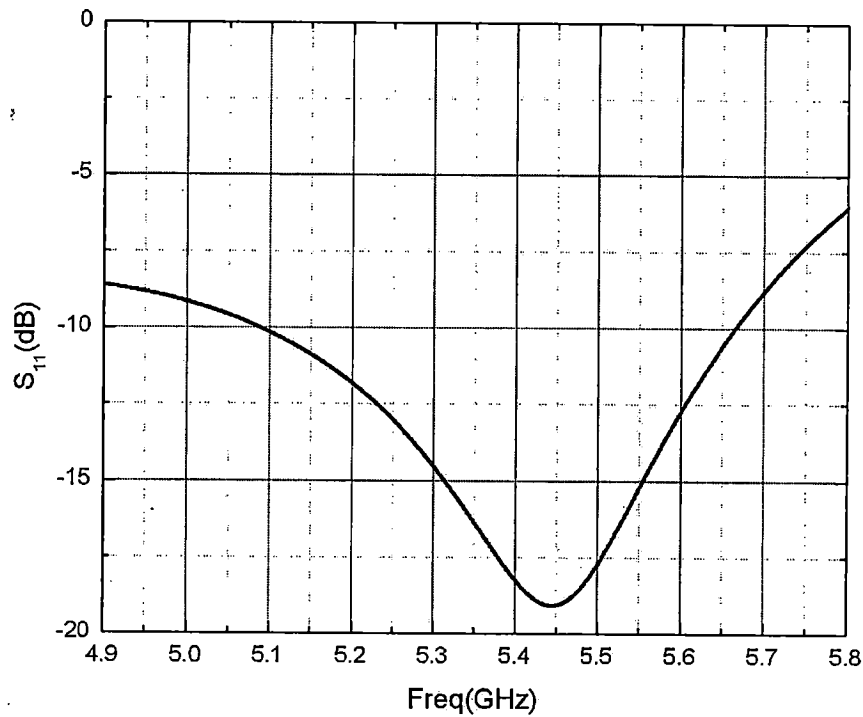


**Fig. 5.8.** Return loss of the slot antenna over EBG surface

### 5.3. PEC backed rectangular-slot antenna

For the PEC backed rectangular slot antenna we need to place the reflector at a distance of  $\lambda/4$  (13 mm) from the antenna. This makes the overall size of the antenna very large. The three dimensional view of the reflector backed rectangular-slot antenna is shown in Fig. 5.9. Its front view is shown in Fig. 5.10 and top view is shown in Fig. 5.11.

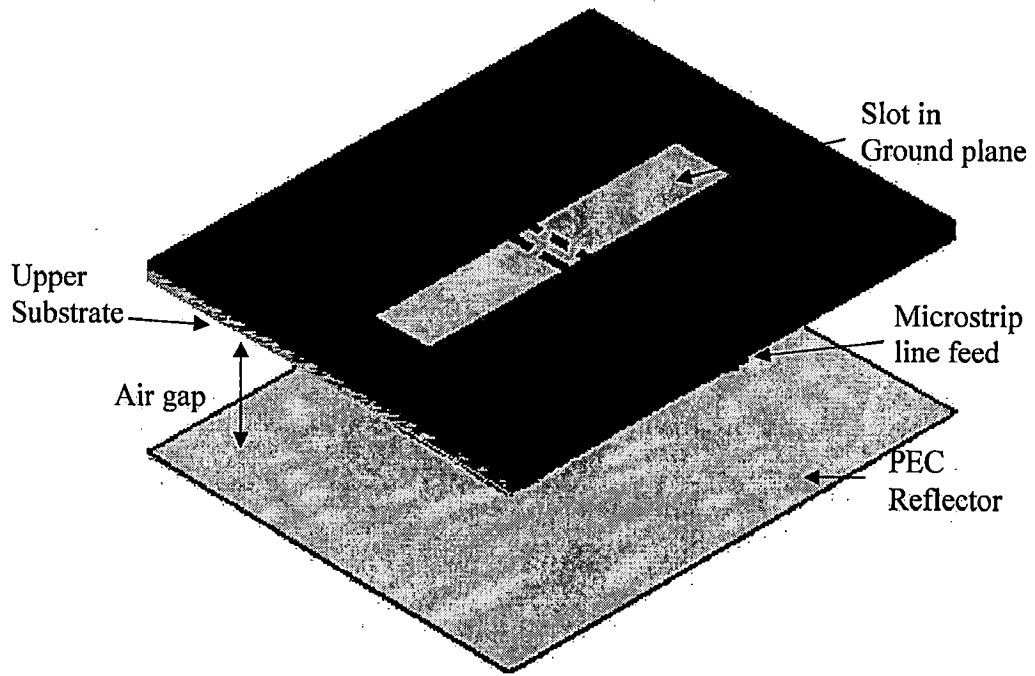


Fig. 5.9. Three dimensional view of the Reflector backed rectangular slot microstrip antenna

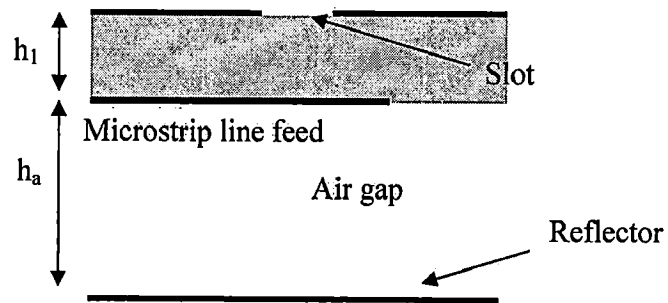


Fig. 5.10. Front view of the Reflector backed rectangular-slot microstrip antenna.

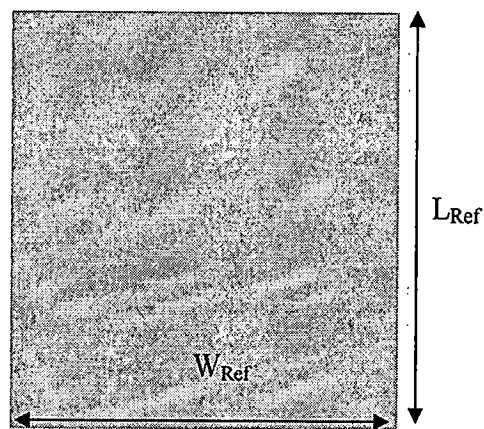
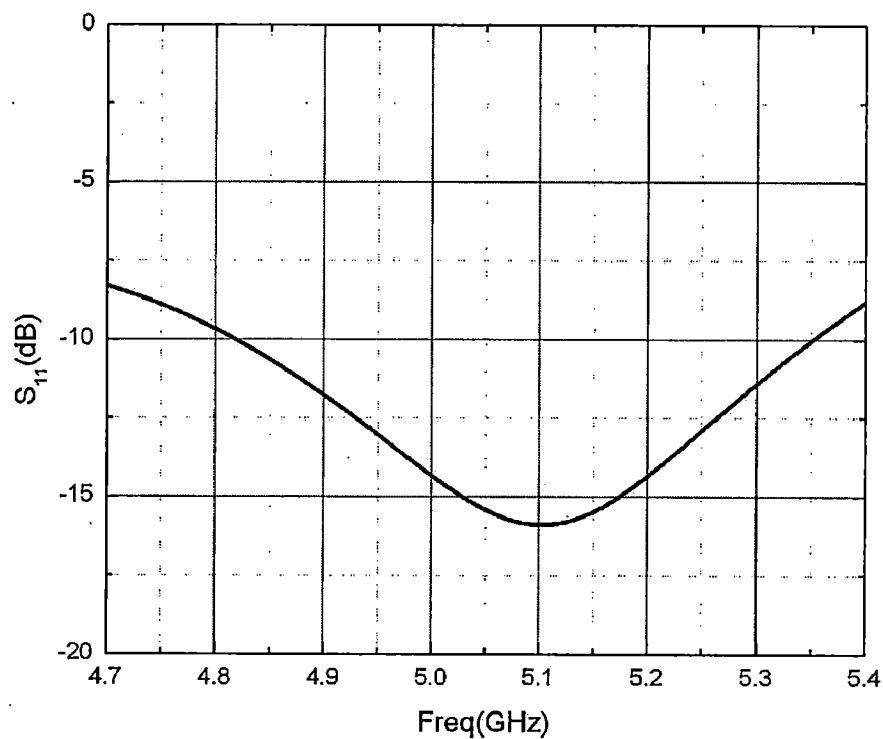


Fig. 5.11. Top view of the Reflector

The tuned parameters for the PEC backed rectangular-slot antenna are shown below:

|   |          |
|---|----------|
| Feed line width ( $W_{msl}$ )                         | 1.146 mm |
| Length of the open circuit stub ( $L_{ocs}$ )         | 7.4 mm   |
| Slot width ( $W_{slot}$ )                             | 4.3 mm   |
| Slot length ( $L_{slot}$ )                            | 28.4 mm  |
| Upper Ground plane width carrying slot ( $W_{gnd}$ )  | 16 mm    |
| Upper Ground plane length carrying slot ( $L_{gnd}$ ) | 36 mm    |
| Lower Reflector width ( $W_R$ )                       | 43.68 mm |
| Lower Reflector length ( $L_R$ )                      | 56.16 mm |
| Air gap ( $h_a$ )                                     | 13 mm    |

The return loss of the antenna with the Reflector surface backing exhibits a resonance at 5.1 GHz and the bandwidth referred to the -10 dB return loss is 10.45%. Fig. 5.12 shows simulated results of the return loss ( $S_{11}$ ) for the Reflector-backed antenna.



**Fig. 5.12. Return loss of the slot antenna over PEC reflector**

#### 5.4. Comparison of the performance of the slot antenna

Fig. 5.13 compares the return loss for all the three cases and Fig. 5.14 compares the gain. As can be seen that both reflector backed as well as EBG backed rectangular slot antenna provides an increase in gain from 2.6 dBi (Reflector case) to 2.9dBi (EBG case) when compared to the unbacked rectangular-slot antenna, which provides a gain of 5.01 dBi.

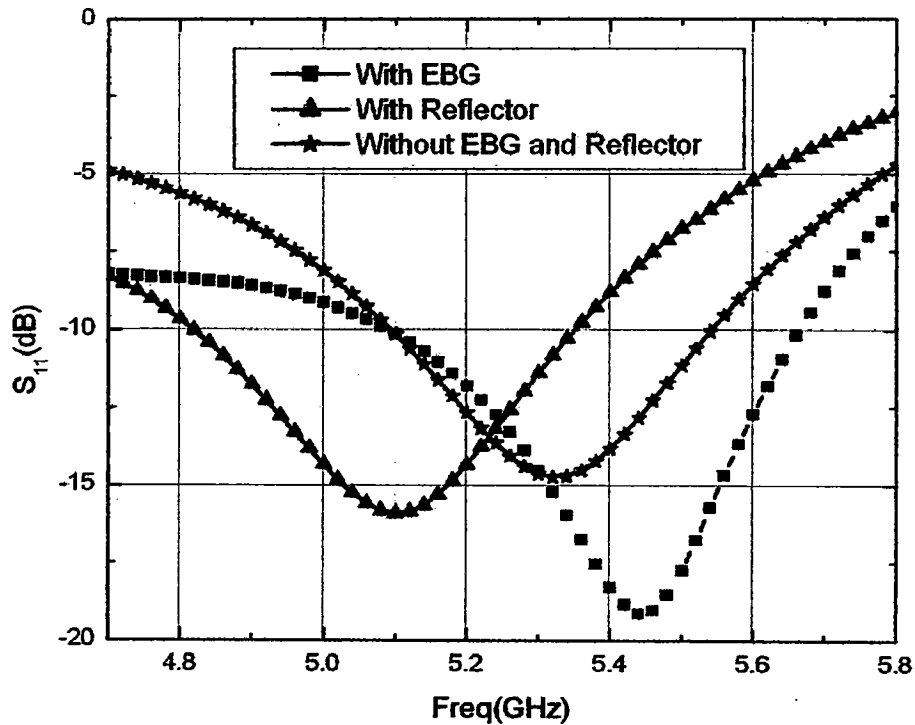


Fig. 5.13. Return Loss of the rectangular-slot antenna with EBG backing, with reflector backing and without EBG and reflector backing.

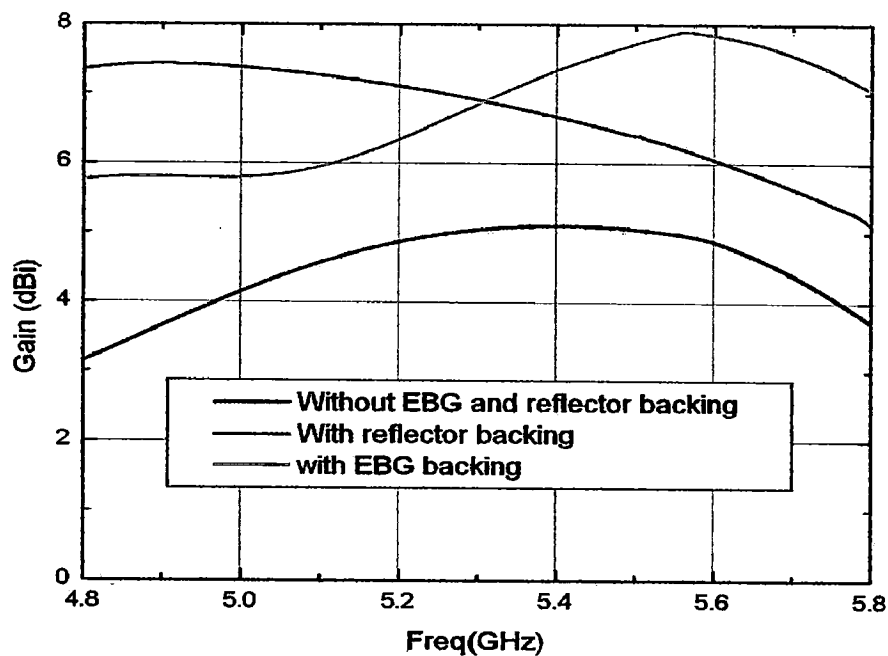
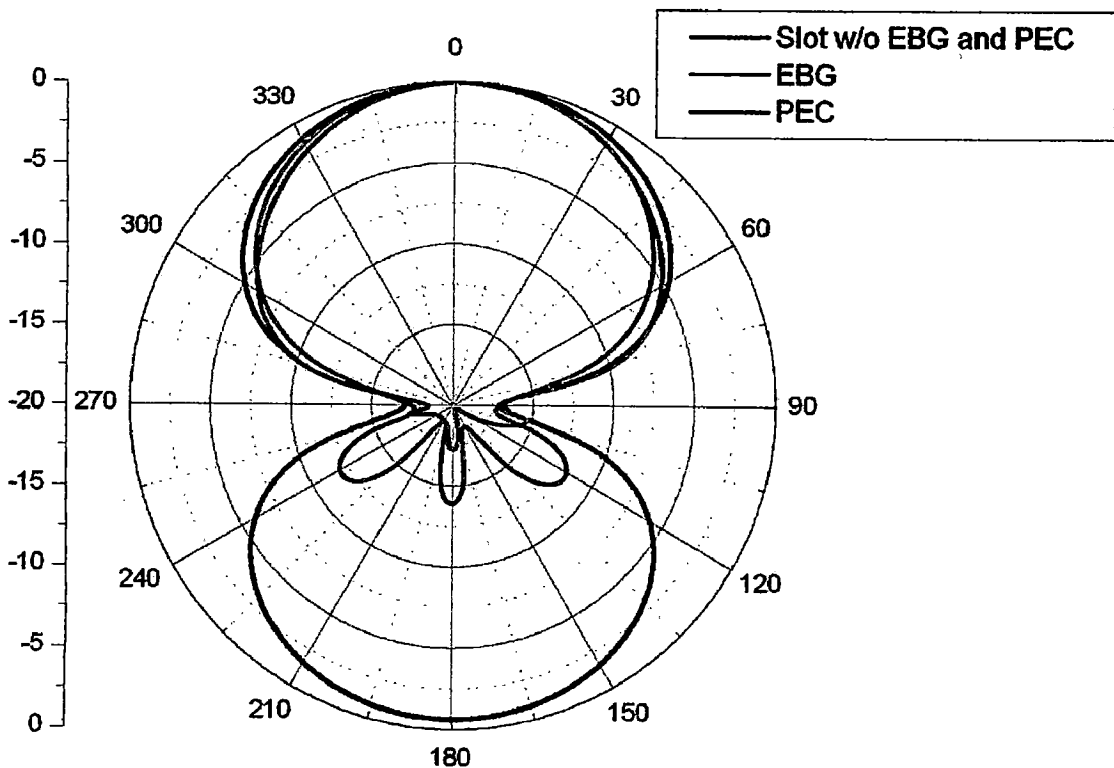


Fig. 5.14. Gain of the rectangular-slot antenna with EBG backing, with reflector backing and without EBG and reflector backing.

## 5.5. Antenna Radiation Pattern Results and Discussion

The goal in this study is the achievement of a uni-directional rectangular slot antenna. Since on a thin substrate, the slot radiates nearly equally on both sides so that the front-to-back ratio is close to 0 dB. Fig. 5.15 shows the comparison of the radiation patterns for the reference rectangular-slot antenna without EBG and PEC backing, with EBG backing and with PEC backing. It is clearly seen that the radiated power is bi-directional for the reference rectangular-slot antenna without EBG and PEC backing.

For the PEC backing antenna, it is seen that the front-to-back ratio is 13.75 dB. In addition, ripples appear in the back-radiated pattern. This relatively low front-to-back ratio is most likely due to radiation of the trapped parallel-plate mode which diffracts from the edges of the plates. Suppression of this mode must be achieved in order to increase the front-to-back ratio and smooth out the patterns.



**Fig. 5.15. Radiation pattern comparison of the slot antenna without EBG backing, with Reflector backing and with EBG backing**

The radiation patterns of the EBG backed rectangular-slot antenna are also depicted in Fig. 5.15. As shown, the front-to-back ratio is 17.18 dB. These results constitute a substantial improvement over the patterns of the PEC backed rectangular-slot antenna. In



addition to the considerably improved front-to-back ratio<sup>8</sup>, compared to the quarter-wavelength backed conducting plate geometry, the EBG backed antenna structure is much more compact as its total thickness is only 5.27 mm compared to 14.27 mm for the quarter-wavelength geometry.

Table 5.1 compares the various parameter of the printed slot antenna for the three cases. It can be seen that there is an improvement in the radiation efficiency for the case of EBG as compared to PEC case. This is because the reflector backing supports the parallel plate mode and power is lost in these modes which considerably reduces the radiation efficiency while for the case of EBG backing, these modes are not allowed to propagate as they lie in the band gap of the EBG structure, Thus, no power loss takes place in EBG case and this results in increase amount of radiation.

**Table 5.1 Comparison of performance of slot antenna with different kind of reflectors**

| Slot antenna                 | Radiation Efficiency | Resonant frequency | S11     |
|------------------------------|----------------------|--------------------|---------|
| Without EBG and ground plane | 95.84 %              | 5.322 GHz          | -14.742 |
| With ground plane            | 86.50 %              | 5.1 GHz            | -15.92  |
| With EBG                     | 91.92 %              | 5.44 GHz           | -19.11  |

## CONCLUSION

---

---

In this work, the design of an electromagnetic band gap structure has been successfully carried out to have a band gap at C band. The proposed structure can be used to reduce the surface wave propagation and as a reflector surface for different printed antennas. Dependence of various performance parameters on the physical parameters of the antenna has been studied. The simulated results of the EBG structure show a band gap from 4.5 GHz to 6.4 GHz.

The presence and extent band gap has been confirmed using three techniques. The theoretically calculated resonant frequency for the band gap structure is 5.12 GHz and 5.42 GHz corresponding to the two edge lengths of the cross shaped patch of the EBG cell. The other two techniques confirm the band gap around this frequency.

Extending this work, the designed EBG has been configured for various antenna applications to enhance their performance parameters.

It has been employed to reduce the mutual coupling between the elements of a 2x1 microstrip patch antenna array and is seen to have reduced the mutual coupling by 13 dB with respect to the structure with no EBG surface.

In order to reduce the geometric profile and to increase the gain of an antenna, EBG surface has been used as a reflector. The profile of the dipole antenna with the EBG surface is seen to have reduced to  $0.105\lambda$  as compared to that of  $0.25\lambda$  for PEC case. This is a significant reduction of 58% on the required profile of the antenna. The gain of the dipole antenna with EBG surface is seen to increase from 1.5 dBi for a dipole without reflector to 8 dBi. The front-to-back lobe ratio is also seen to improve by a factor of 5dB as compared to the PEC case.

In another application, EBG surfaces have been employed with slot antenna structure. The height of the slot antenna is seen to have reduced from  $0.25\lambda$  as is required when a PEC is used as reflector to  $0.095\lambda$ . This is a significant reduction of 62% on the required profile of the antenna. The gain of the slot antenna with EBG surface is seen to increase from approximately 5.5 dBi for the slot antenna without any reflector to 8 dBi. The front-

## **FUTURE SCOPE**

---

---

- This EBG surface can also be used in other application such as in waveguide in order to make the field distribution uniform along the cross section of the waveguide.
- Higher band gap EBG structures can be developed using multi layer structures.
- This EBG structure can also be employed for the development of duplexer.
- Second and higher order band gaps can be studied for their usefulness in different applications.
- This EBG structures can also be used with band pass filter to suppress higher order modes.

## REFERENCES

---

---

- [1] A. R. Weily, L. Horvath, K. P. Esselle, B. C. Sanders and T. S. Bird, "A Planar Resonator Antenna Based on a Woodpile EBG Material", *IEEE Transactions On Antennas And Propagation*, vol. 53, No. 1, pp. 216-223, January 2005.
- [2] R. Gonzalo, P. D. Maagt and M. Sorolla, "Enhanced patch-antenna performance by suppressing surface waves using photonic bandgap substrates", *IEEE Trans. MTT*, vol. 47, No. 11, pp. 2131-2139, November 1999.
- [3] T. H. Liu, W. X. Zhang, M. Zhang and K. F. Tsang, "Low profile spiral antenna with PBG substrate," *Electron. Lett.*, vol. 36, no. 9, pp. 779-780, Apr. 2000.
- [4] F. Yang and Y. Rahmat-Samii, "A low profile circularly polarized curl antenna over electromagnetic band-gap (EBG) surface," *Microwave Opt. Technol. Lett.*, vol. 31, no. 3, pp. 165-168, 2001.
- [5] K. P. Ma, F. R. Yang, Y. Qian and T. Itoh, "Nonleaky conductor-backed CPW using a novel 2-D PBG lattice," in *Asia-Pacific Microwave Conf. Dig.*, Dec. 1998, pp. 509-512.
- [6] K. P. Ma, J. Kim, F. R. Yang, Y. Qian and T. Itoh, "Leakage suppression in stripline circuits using a 2-D photonic bandgap lattice," in *IEEE MTT-S Microwave Symp. Dig.*, Anaheim, CA, June 13-19, 1999, pp. 73-76.
- [7] K. P. Ma, K. Hirose, F. R. Yang, Y. Qian and T. Itoh, "Realization of magnetic conducting surface using novel photonic bandgap structure," *Electron. Lett.*, vol. 34, pp. 2041-2042, Nov. 1998.
- [8] F. R. Yang, K. P. Ma, Y. Qian and T. Itoh, "A novel TEM waveguide using uniplanar compact photonic-bandgap (UC-PBG) structure," *IEEE Trans. Microwave Theory Tech.*, vol. 47, pp. 2092-2098, Nov. 1999.
- [9] G. P. Gauthier, A. Courta y and G. M. Rebeiz, "Microstrip antennas on synthesized low dielectric-constant substrates", *IEEE Trans. on Antennas and Propagation.*, vol. 45, pp. 1310-1314, Aug. 1997.
- [10] V. Radisic, Y. Qian, R. Coccioli and T. Itoh, "A novel 2-D photonic band-gap structure for microstrip lines", *IEEE Microwave Guided Wave Lett.*, vol. 8, pp. 69-71, Feb. 1998.

- [11] R. Coccioli, W. R. Deal and T. Itoh, "Radiation characteristics of a patch antenna on a thin PBG substrate", presented at the *IEEE AP-S Int. Symp.*, Atlanta, GA, pp. 21–26, June 1998.
- [12] K. M. Ho, C. T. Chan, C. M. Soukoulis, R. Biswas and M. Sigalas, "Photonic band gaps in three dimensions: New layer-by-layer periodic structures," *Solid State Commun.*, vol. 89, no. 5, pp. 413–416, 1994.
- [13] H. Mosallaei and K. Sarabandi, "Magneto-Dielectrics in Electromagnetics: Concept and Applications" *IEEE Transactions on Antennas And Propagation*, Vol. 52, No. 6, pp. 1558-1567, June 2004.
- [14] D.F. Sievenpiper, "High-Impedance Electromagnetic Surfaces", *PhD Dissertation, Dept. Electrical Engineering, 1999, University Of California, Los Angeles.*
- [15] Y. Qian, R. Coccioli, D. Sievenpiper, V. Radisic, E. Yablonovitch and T. Itoh, "Microstrip patch antenna using novel photonic band-gap structures", *Microwave J.*, vol. 42, no. 1, pp. 66–76, Jan. 1999.
- [16] F. Yang, K. Ma, Y. Qian and T. Itoh, "A uniplanar compact photonic bandgap (UC-PBG) structure and its application for microwave circuits", *IEEE Trans. Microwave Theory Tech.*, vol. 47, pp. 1509–1514, Aug. 1999.
- [17] K. P. Ma, F. R. Yang, Y. Qian and T. Itoh, "Nonleaky conductor-backed CPW using a novel 2D-PBG lattice," *presented at the Asia-Pacific Microwave Conf., Yokohama, Japan, Dec. 8–11, 1998.*
- [18] F. R. Yang, Y. Qian, R. Coccioli and T. Itoh, "A novel low loss slowwave microstrip structure," *IEEE Microwave Guided Wave Lett.*, vol. 8, pp. 372–374, Nov. 1998.
- [19] R. Coccioli, F. R. Yang, K. P. Ma and T. Itoh, "Aperture-Coupled Patch Antenna on UC-PBG Substrate", *IEEE Trans. on Microwave theory and Techniques*, vol. 47, No. 11, pp. 2123-2130, November 1999.
- [20] D. J. Kern, S. H. Werner, A. Monorchio, L. Lanuzza and M. J. Wilhelm, "The Design Synthesis of Multiband Artificial Magnetic Conductors Using High Impedance Frequency Selective Surfaces", *IEEE Trans. on Antennas and Propagation.*, vol. 53, No. 1, pp. 8-17, Jan. 2005.
- [21] Y. Rahmat-Samii and F. Yang, "Microstrip Antenna Integrated with Electromagnetic band-gap (EBG) structures: A Low mutual coupling design for

- array applications”, *IEEE Trans. on Antennas and Propagation*, vol. 51, No. 10, pp. 2936-2946, October 2003.
- [22] Z. Li and Y. Rahmat-Samii, “PBG, PMC and PEC surface for antenna applications: A comparative study”, in *Proc. IEEE AP-S Dig.*, pp. 674–677, July 2000.
- [23] F. Yang and Y. Rahmat-Samii, “Reflection phase Characterizations of an EBG Ground Plane for Low Profile Wire Antenna Applications”, *IEEE Trans. on Antennas and Propagation.*, vol. 51, No. 10, pp. 2691-2703, October. 2003.
- [24] F. Yang and Y. Rahmat-Samii, “Reflection phase characterization of an electromagnetic band-gap (EBG) surface”, in *Proc. IEEE AP-S Dig.*, vol. 3, pp. 744–747, June 2002.
- [25] P. Raumonon, M. Keskilammi, L. Sydanheimo, M. Kivikoski “A Very Low Profile CP EBG Antenna for RFID Reader”, *IEEE Antennas and Propagation Society Symposium*, vol. 4, pp. 3808 – 3811, June 2004.
- [26] F. Yang and Y. R. Sammi, “Applications of Electromagnetic Band-Gap (EBG) Structures in Microwave Antenna Designs”, *IEEE 3<sup>rd</sup> International Conference on Microwave and Millimeter Wave Technology Proceedings*, pp. 528-531, 2002.
- [27] M. Fallah-Rad and I. Shafai “Enhanced Performance of a Microstrip Patch Antenna using a High Impedance EBG Structure”, *IEEE Antennas and Propagation Society International Symposium*, vol. 3, pp. 982 – 985, June 2003.
- [28] S. K. Sharma and L. Shafai “Enhanced Performance of an Aperture coupled Rectangular Microstrip Antenna on a Simplified Unipolar Compact Photonic Bandgap (UC-EBG) Structure” *IEEE Antennas and Propagation Society International Symposium, 2001*, vol. 2, 8-13, pp. 498 – 501, July 2001.
- [29] L. Yang, M. Fan F. Chen, J. She and Z. Feng, “A Novel Compact Electromagnetic-Bandgap(EBG) Structure and Its Applications for Microwave Circuits”, *IEEE Trans. on Microwave theory and Techniques*, vol. 53, No. 1, pp. 183-190, January 2005.
- [30] L. Yang, M. Fan F. Chen, J. She and Z. Feng, “A Novel Compact Electromagnetic Band-gap (EBG) Structure and its Application in Microstrip Antenna Arrays”, *IEEE MTT-S Digest 2004*.
- [31] F. Elek, R. Abhari and G. V. Eleftheriades, “A Uni-Directional ring-Slot Antenna Achieved by Using an Electromagnetic Band-Gap Surface”, *IEEE Transactions On Antennas And Propagation*, vol. 53, No. 1, pp. 181-190, January 2005.

- [32] G. P. Gauthier, A. Courtay and G. H. Rebeiz, "Microstrip antennas on synthesized low dielectric-constant substrate," *IEEE Trans. Antennas Propagat.*, vol. 45, pp. 1310–1314, Aug. 1997.
- [33] I. Papapolymerou, R. F. Frayton and L. P. B. Katehi, "Micromachined patch antennas," *IEEE Trans. Antennas Propagat.*, vol. 46, pp. 275–283, Feb. 1998.
- [34] J. S. Colburn and Y. Rahmat-Samii, "Patch antennas on externally perforated high dielectric constant substrates," *IEEE Trans. Antennas Propagat.*, vol. 47, pp. 1785–1794, Dec. 1999.
- [35] D. H. Schaubert and K. S. Yngvesson, "Experimental study of a microstrip array on high permittivity substrate," *IEEE Trans. Antennas Propagat.*, vol. 34, pp. 92–97, Jan. 1986.
- [36] D. H. Schaubert, D. M. Pozar and A. Adrian, "Effect of microstrip antenna substrate thickness and permittivity: Comparison of theories with experiment," *IEEE Trans. Antennas Propagat.*, vol. 37, pp. 677–682, June 1989.